J Atmos Chem (2007) 57:171–202
DOI 10.1007/s10874-007-9071-0

Evaluation of α- and β-pinene degradation in the detailed tropospheric chemistry mechanism, MCM v3.1, using environmental chamber data

P. G. Pinho · C. A. Pio · W. P. L. Carter · M. E. Jenkin

Received: 12 October 2006 / Accepted: 5 April 2007 /
Published online: 8 May 2007

Abstract The representation of the degradation of the monoterpenes, α- and β-pinene, in version 3.1 of the Master Chemical Mechanism (MCM v3.1) has been evaluated, using environmental chamber data from the Statewide Air Pollution Research Center (SAPRC) at the University of California. As part of this evaluation, a representation of the reactions of the monoterpenes with $O(^3P)$ has also been included, these reactions being significant under chamber conditions but generally insignificant under atmospheric conditions. The results demonstrate that MCM v3.1 provides a consistent description of the photo-oxidation of α-pinene/NO_X mixtures for a range of initial VOC/NO_X, but with the formation rate of ozone and decay rate of α-pinene generally being overestimated. Sensitivity of the system to parameter uncertainties and mechanistic variations proposed in the literature are described. The collective implementation of a number of refinements allows the simulations to be brought into good agreement with the experimental observations for the complete series of experiments, with each of the refinements being consistent with reported parameter uncertainty ranges or mechanistic adjustments. The system is particularly sensitive to the magnitudes of sources and sinks of free radicals. The impacts of several other reported mechanistic variations which potentially influence the first generation product distribution and the ozone formation chain length of the initial oxidation step are also described and assessed. MCM v3.1 is shown to provide a reasonable, but less consistent, description of photo-oxidation of β-pinene/NO_X mixtures. The simulated magnitudes of the ozone formation rates and β-pinene removal rates are broadly comparable with the experimental

P. G. Pinho · C. A. Pio
CESAM & Department of Environment, University of Aveiro, 3800-193 Aveiro, Portugal

W. P. L. Carter
Center for Environmental Research and Technology, College of Engineering, University of California, Riverside, CA 92521, USA

M. E. Jenkin (✉)
Centre for Environmental Policy, Imperial College London, Silwood Park, Ascot, Berkshire SL5 7PY, UK
e-mail: m.jenkin@imperial.ac.uk

observations, but the mechanism tends towards overestimation of ozone formation at low VOC/NO_X and underestimation at high VOC/NO_X. Implementation of a number of mechanistic variations reported in the literature does not allow the associated simulations to be brought into good agreement with the observations for the entire VOC/NO_X range. The system is particularly sensitive to changes which influence the formation of HCHO (and resultant radical production upon its photolysis), and the impacts of the tested mechanistic variations are usually dominated by this effect. As a result of this work, gaps and uncertainties in the kinetic, mechanistic and chamber database for the monoterpenes are identified and discussed.

Keywords VOC oxidation · α-pinene · β-pinene · Tropospheric chemistry · Degradation mechanisms · Environmental chamber data · Ozone modelling

1 Introduction

It is well established that degradation of emitted volatile organic compounds (VOC) has a major influence on the chemistry of the lower atmosphere (e.g. Leighton 1961; Finlayson-Pitts and Pitts 2000; Atkinson 2000; Jenkin and Clemitshaw 2000), contributing to the formation of ozone and other secondary pollutants which may have harmful impacts on human health and on the environment (e.g. PORG 1997).

Monoterpenes are a class of VOC of empirical formula $C_{10}H_{16}$, which are ubiquitous in the lower troposphere. They are of natural origin, being emitted by vegetation, namely coniferous plants as well as members of the families *Lami-aceae, Apiaceae, Rutaceae, Myrtaceae and Asteraceae, Quercus Ilex and Quercus robur* (e.g. Kesselmeier and Staudt 1999 and references therein). Emission rates are species and seasonally dependent, and increase exponentially with temperature, with annual global emissions estimated to be 127 Tg C $year^{-1}$ (e.g., Guenther et al. 1995). As result of their large emission rates and their generally high chemical reactivity, monoterpenes play an important role in atmospheric chemistry, principally in non-urban areas, on regional and global scales. Although a large number of emitted monoterpenes have been identified, particular emphasis has been placed on α- and β-pinene, since measurements of monoterpene speciation suggest that these make a particularly significant contribution to global monoterpenes emissions (e.g., Guenther et al. 1994 and references therein), and also because they are representative of classes of monoterpene having either a cyclic double bond (in the case of α-pinene) or an exocyclic double bond (in the case of β-pinene). Consequently, various representations of their degradation have been included in atmospheric models used for research or regulatory purposes.

There are a large number of condensed chemical reaction mechanisms to describe and represent the atmospheric chemical transformations of emitted VOC. On the contrary, only a very limited number of mechanisms exist with a detailed description of chemical transformation processes for primary and secondary atmospheric species. One example is the Master Chemical Mechanism (MCM) (Jenkin et al. 1997), which is a near-explicit chemical mechanism that describes the detailed degradation of a series of emitted VOC, and the resultant generation of ozone and other secondary pollutants, under conditions appropriate to the planetary boundary layer. The philosophy behind the construction of MCM is to apply available experimental and theoretical information on the kinetics and products of elementary reactions relevant to VOC oxidation, in order to build up a near-explicit representation of the tropospheric degradation processes. A fundamental assumption in the

mechanism construction, therefore, is that the kinetics and products of a large number of unstudied chemical reactions can be defined on the basis of the known reactions of a comparatively small number of similar chemical species, by analogy and with the use of structure-reactivity correlations (Jenkin et al. 1997, 2003; Saunders et al. 2003; Bloss et al. 2005). Version 3.1 of the Master Chemical Mechanism (MCM v3.1) considers the oxidation of 135 primary VOC. The complete mechanism comprises ca. 13,500 reactions of ca. 5,900 species, which were defined on the basis of the MCM scheme writing protocols (Jenkin et al. 1997, 2003; Saunders et al. 2003; Bloss et al. 2005). The MCM can be accessed at, and downloaded from, the website: http://mcm.leeds.ac.uk/MCM.

In addition to its application to the examination of detailed chemical processing on local and regional scales (e.g., Derwent et al. 2005; Utembe et al. 2005; Johnson et al. 2006a,b), the MCM is also increasingly being used as a benchmark mechanism for the development and/or testing of reduced chemical mechanisms for use in local, regional and global scale models requiring more economical representations of chemical processing (e.g., Poschl et al. 2000; Jenkin et al. 2002; Whitehouse et al. 2004a,b; Bonn et al. 2004). It is therefore desirable that the performance of the MCM is evaluated, where possible, using the results of environmental chamber experiments. A number of previous studies have used the results of experiments from the European Photoreactor (EUPHORE) to evaluate the performance of the MCM v3.1 degradation schemes for α-pinene (Saunders et al. 2003), benzene, toluene, *p*-xylene and 1,3,5-trimethylbenzene (Bloss et al. 2005) and ethene (Zádor et al. 2005); data from the Statewide Air Pollution Research Center (SAPRC) chambers to evaluate the performance of the MCM v3.1 degradation schemes for butane and isoprene, and their oxidation products formaldehyde, acetaldehyde, methylethyl ketone, methacrolein and methylvinyl ketone (Pinho et al. 2005), and ethene, propene, 1-butene and 1-hexene (Pinho et al. 2006); and data from the CSIRO indoor chamber to evaluate the performance of the MCM v3.1 degradation schemes for propene and 1-butene (Hynes et al. 2005). As part of this ongoing process, the present study also makes use of the large SAPRC dataset to evaluate the MCM v3.1 degradation mechanisms for α- and β-pinene. This work extends substantially the range VOC/NO_X ratios considered in the EUPHORE α-pinene appraisal of Saunders et al. (2003), which focused on very high VOC/NO_X ratios, and represents the first evaluation of the β-pinene mechanism. The sensitivity of the systems to a number of parameter uncertainties and proposed mechanistic variations reported in the literature are considered, and a series of modifications are identified for possible inclusion in future releases of the MCM. As a result of this work, gaps and uncertainties in the kinetic, mechanistic and chamber database are also identified and discussed.

2 Chamber data

The mechanistic evaluation has been carried out using the database of the SAPRC indoor chambers. The set of computer data files containing the environmental chamber data can be obtained on the Internet for the experiments documented by Carter et al. (1995a), at the address given with that citation below.

Data from the following environmental chambers were used in the present evaluation: Indoor Teflon Chamber no. 2 (ETC); Dividable Teflon Chamber (DTC); and Xenon Arc Teflon Chamber (XTC). As described in detail elsewhere (e.g., Carter 2000) these chambers are built in Teflon, and vary in volume from 2,500 to 6,400 dm^3. The ETC and DTC chambers are illuminated using blacklights. The available datasets from the above chambers

were used previously in the development and evaluation of the SAPRC-99 mechanism (Carter 2000), and in the previous appraisals of isoprene, butane and alkene degradation (Pinho et al. 2005, 2006).

The set of chamber experimental runs employed in the present evaluation consisted of a database of six α-pinene-NO_X-air, six β-pinene-NO_X-air and five acetone-NO_X-air experiments. The range of reagent concentrations for the considered experiments is presented in Table 1. Full details of the experimental conditions and reagent concentrations are available elsewhere (Carter et al. 1995a; Carter 2000), which include detailed documentation of the measurement uncertainties associated with the analytical methods employed for the reactants and products, and the precision and accuracy of other experimental parameters (e.g. temperature; light intensity and spectrum of photolysing radiation).

Auxiliary mechanisms representing the impact of wall effects in each of the chambers have been optimised previously using data from butane-NO_X photo-oxidation experiments (Pinho et al. 2005), and these are applied in the present study. The rates applied to photolysis processes were based on spectral distributions and absolute light intensities which are fully documented for all the SAPRC chambers (e.g. Carter et al. 1995a,b).

3 Chemistry of α- and β-pinene degradation in MCM v3.1

The complete degradation chemistry, as represented in MCM v3.1, consists of: 925 reactions of 321 species for α-pinene; and 1,149 reactions of 400 species for β-pinene (a combined scheme degrading both α- and β-pinene consists of 1,550 reactions of 536 species). The chemistry can be viewed and downloaded using the subset mechanism assembling facility, available as part of the MCM website. The methodology of mechanism construction has been described in detail by Saunders et al. (2003), with chemistry initiated by reaction with OH, O_3 and NO_3 represented in each case. Salient features of the OH and O_3-initiated chemistry are now summarized. For the photo-oxidation conditions considered here, the systems are insensitive to the NO_3-initiated chemistry which is therefore not discussed further.

The main features of the OH-initiated degradation chemistry to first generation products when NO_X is present are summarized in Fig. 1. This demonstrates that oxidation of both α- and β-pinene in MCM v3.1 proceeds by sequential addition of OH and O_2 leading, in each case, to the initial formation of three isomeric hydroxyl-substituted peroxy radicals (RO_2). Addition of OH at the more substituted sites, followed by O_2 addition, leads to the formation of the secondary and primary radicals, APINBO2 and BPINBO2. Addition of OH at the less-substituted sites generates hydroxy-substituted tertiary organic radicals, which are assumed to isomerise partially prior to O_2 addition, following the mechanism

Table 1 Ranges of reagent concentrations, relative humidities and NO_2 photolysis constants (k_6) for the considered experiments

	α-pinene-NOx	β-pinene-NOx	Acetone-NOx
No. of available runs	6	6	5
[VOC] (ppm)	0.263–0.445	0.265–0.968	8.461–15.000
[NOx] (ppm)	0.132–0.534	0.137–0.293	0.137–0.286
[VOC]/[NOx]	0.523–2.128	0.946–3.301	37.338–102.810
k_6 (min^{-1})	0.252–0.351	0.251–0.351	0.254–0.388
Relative humidity	<5%	<5%	<5%

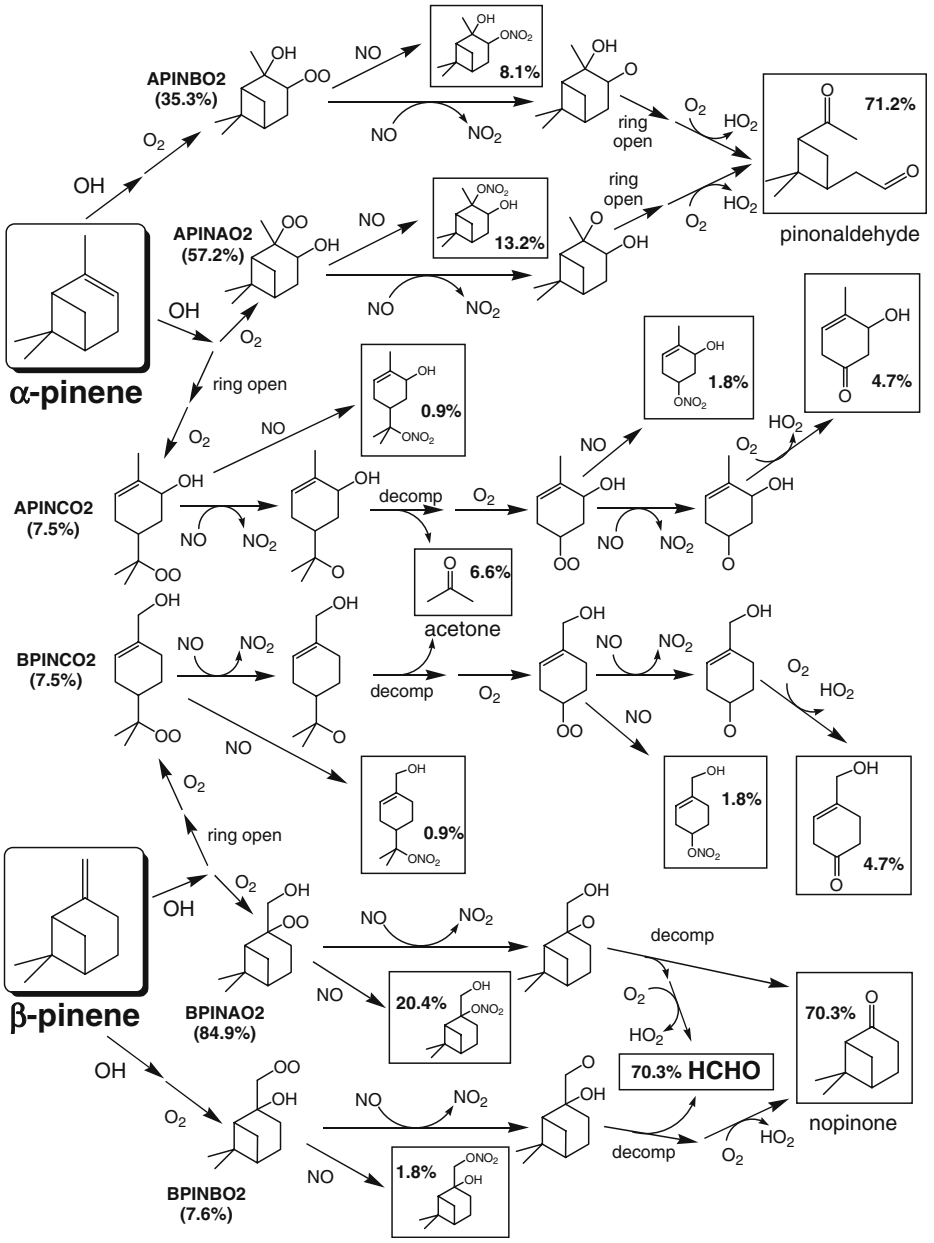

Fig. 1 Schematic of the main features of the OH-initiated degradation of α- and β-pinene to first generation products in the presence of NO_X, as represented in MCM v3.1

suggested by Nozière et al. (1999) and Vereecken and Peeters (2000) for α-pinene. The importance of the isomerisation mechanism is set such that the primary yield of the isomerised radicals (APINCO2 and BPINCO2) is 7.5%, this constraint being guided by the yields of acetone reported in the literature (see below). In each case, therefore, the

hydroxy-substituted tertiary organic radicals mainly react with O_2 (i.e., in preference to isomerisation) to generate the major radicals APINAO2 and BPINAO2 (see Fig. 1). As described by Saunders et al. (2003), the initial OH addition ratios applied in MCM v3.1 were estimated using the SAR method of Peeters et al. (1994). More recently Peeters et al. (2001) and Capouet et al. (2004) have calculated and applied substantially modified ratios for the initial RO_2 radical distribution. This is considered further below in the sensitivity studies (Sections 4.2 and 4.3).

The subsequent chemistry in the presence of NO_X leads predominantly to the formation of carbonyl products, with their subsequent oxidation leading ultimately to the formation of CO and CO_2. At each oxidation stage, the chemistry is propagated by reactions of peroxy (RO_2) and oxy (RO) radical intermediates. For example, the initial oxidation sequence involving BPINAO2 proceeds via the following catalytic cycle:

$$\mathrm{OH} + \beta\text{-pinene}(+\mathrm{O_2}) \rightarrow \mathrm{BPINAO2} \tag{1}$$

$$\mathrm{BPINAO2} + \mathrm{NO} \rightarrow \mathrm{BPINAO} + \mathrm{NO_2} \tag{2}$$

$$\mathrm{BPINAO} \rightarrow \mathrm{nopinone} + \mathrm{CH_2OH} \tag{3}$$

$$\mathrm{CH_2OH} + \mathrm{O_2} \rightarrow \mathrm{HCHO} + \mathrm{HO_2} \tag{4}$$

$$\mathrm{HO_2} + \mathrm{NO} \rightarrow \mathrm{OH} + \mathrm{NO_2} \tag{5}$$

The peroxy radicals (RO_2 and HO_2) thus provide the coupling with the chemistry of NO_X, which leads to NO-to-NO_2 conversion, and formation of O_3 upon photolysis of NO_2:

$$\mathrm{NO_2} + \mathrm{h}\upsilon \rightarrow \mathrm{NO} + \mathrm{O}\left(^3\mathrm{P}\right) \tag{6}$$

$$\mathrm{O}\left(^3\mathrm{P}\right) + \mathrm{O_2}(+\mathrm{M}) \rightarrow \mathrm{O_3}(+\mathrm{M}) \tag{7}$$

The subsequently-formed oxy radicals determine the identity or identities of the carbonyl products generated from the degradation. In MCM v3.1, the radicals APINAO, APINBO, BPINAO and BPINBO are assumed to undergo exclusive C–C bond scission, leading to the formation of the major carbonyl products, pinonaldehyde (in the case of α-pinene) and nopinone and HCHO (in the case of β-pinene), resulting in molar yields of ca. 70% in each case from the NO_X-propagated chemistry. These are generally at the high end of the yield ranges reported in the literature (Arey et al. 1990; Hatakeyama et al. 1991; Hakola et al. 1994; Nozière et al. 1999; Wisthaler et al. 2001; Aschmann et al. 2002a): (28–87%) for pinonaldehyde; (25–79%) for nopinone; (45–54%) for HCHO. A number of studies have considered potentially competing 1,5-H atom shift isomerisation reactions for the above oxy radicals, particularly in relation to the observed formation of HCHO as a first generation product of α-pinene oxidation (Aschmann et al. 1998; Orlando et al. 2000; Peeters et al. 2001) and also to consider their effect on OH radical recycling in both terpene systems (Davis and Stevens 2005; Davis et al. 2005). Similarly, Nozière et al. (1999) postulated competitive decomposition of APINAO by ejection of the CH_3 group as a

possible route to first generation HCHO formation. The impact of these mechanisms is considered further below in the sensitivity studies (Sections 4.2 and 4.3).

The radicals APINCO and BPINCO are also assumed to undergo exclusive C–C bond scission in MCM v3.1, leading in each case to the formation of acetone and an unsaturated hydroxy-substituted C_7 cyclic radical. The resultant yield of acetone from the NO_X-propagated chemistry in both terpene systems (6.6%) is consistent with the ranges reported in the literature (Gu et al. 1984; Aschmann et al. 1998; Nozière et al. 1999; Orlando et al. 2000; Wisthaler et al. 2001): (5–15%) for α-pinene; (2–13%) for β-pinene. As shown in Fig. 1, the cyclic radicals, formed in conjunction with acetone, are assumed to be oxidised mainly to form unsaturated hydroxycycloketone products, via conventional reactions of the corresponding RO_2 and RO intermediates with NO and O_2, respectively.

The further degradation of the first (and subsequent) generation carbonyl products by reaction with OH, leads to further NO-to-NO_2 conversion (and therefore O_3 formation). Consequently, the number of NO-to-NO_2 conversions at each oxidation step, and the lifetimes of the parent terpene and its product carbonyls (which are partially determined by their OH reactivity) have an influence on the rate of NO oxidation and O_3 formation. Whereas the chemistry of the simple carbonyl products (i.e., HCHO and acetone) is well established (and represented in MCM v3.1), there is comparatively little experimental information on the oxidation mechanisms of the more complex species, in particular the major products pinonaldehyde and nopinone. Their degradation is therefore based on the generic rules described in the MCM protocols (Jenkin et al. 1997; Saunders et al. 2003). In the case of pinonaldehyde, the NO_X-propagated degradation chemistry (via two H atom abstraction channels), follows two sequences, each leading to the ultimate formation of HCHO, acetone and a C_5 tricarbonyl. Because these sequences include a number of isomerisation and decomposition/ring-opening steps, and thus each involve five intermediate RO_2 radicals (and NO-to-NO_2 conversions), the oxidation of pinonaldehyde into these second generation products is comparatively efficient at generating ozone. A more detailed theoretical appraisal of the OH initiated degradation of pinonaldehyde has been performed by Fantechi et al. (2002), and subsequently applied by Capouet et al. (2004). The impacts of this appraisal on the present chamber simulations are considered in the sensitivity studies described below (Section 4.2).

The NO_X propagated degradation chemistry of nopinone in MCM v3.1 proceeds via four H atom abstraction channels. Similarly to pinonaldehyde, a substantial proportion (ca. 80%) of this chemistry follows reaction sequences with a number of isomerisation and decomposition/ring-opening steps, leading to the formation of acetone and C_6 tricarbonyl co-products. However, a notable proportion (ca. 20%) proceeds via a short reaction sequence, in which the relevant RO radical partially reacts with O_2 to generate a diketone product (6,6-dimethyl-bicyclo[3.1.1]heptane-2,4-dione) which retains the bicyclic carbon skeleton. This latter sequence is thus comparatively inefficient a generating ozone, both intrinsically, and also because the bicyclic diketone product is estimated to be of lower reactivity than nopinone by a factor of ca. 3. Lewis et al. (2005) have recently carried out a detailed theoretical appraisal of the OH attack distribution on nopinone, and the impact of results of this appraisal on the present chamber simulations is considered in the sensitivity studies described below (Section 4.3).

The chemistry discussed above, and represented in reactions (1–5), consists entirely of propagation reactions which conserve the radical population in the system. The organic degradation chemistry can also influence oxidation rates, and therefore O_3 formation, through either producing or removing radicals, and such processes have generally been shown to have a major influence on mechanism performance in previous appraisals of the

MCM using environmental chamber data (e.g., Pinho et al. 2005, 2006). The photolysis of carbonyl compounds is a potential source of free radicals, which may have an important influence. Of relevance to the current systems is the photolysis of the simple carbonyls, HCHO and acetone, and of some of the more complex carbonyls, such as pinonaldehyde and related species. Absorption cross-section and quantum yield data are available for the simple species, for which the following radical-forming photolysis channels are represented in MCM v3.1:

$$\mathrm{HCHO} + h\upsilon\ (+2\mathrm{O_2}) \rightarrow \mathrm{CO} + \mathrm{HO_2} + \mathrm{HO_2} \tag{8}$$

$$\mathrm{CH_3COCH_3} + h\upsilon\ (+2\mathrm{O_2}) \rightarrow \mathrm{CH_3C(O)O_2} + \mathrm{CH_3O_2} \tag{9}$$

On the basis of chamber photo-oxidation data, the photolysis parameters assigned to HCHO have been tested (and refined) previously (Pinho et al. 2005), and the representation of acetone photolysis is similarly tested below (Section 4.1). Pinonaldehyde photolysis is also assumed to lead to radical formation (via the Norrish "Type I" process), in accordance with the following overall reaction in air (where R′ represents the 3-acetyl-2,2-dimethyl-cyclobutyl group):

$$\mathrm{R'CH_2CHO} + h\upsilon\ (+2\mathrm{O_2}) \rightarrow \mathrm{R'CH_2O_2} + \mathrm{CO} + \mathrm{HO_2} \tag{10}$$

The sensitivity of the α-pinene simulations to this assumption, and the implementation of molecular product channels for pinonaldehyde and related species, is discussed further below (Section 4.2). In addition to carbonyl photolysis, photolysis reactions are generally included in MCM v3.1 schemes for products containing nitrate, hydroperoxide and peracid functionalities, as described by Jenkin et al. (1997) and Saunders et al. (2003).

At the typical concentrations of NO_X in chamber experiments, the reactions of intermediate peroxy radicals with either NO or NO_2 may contribute to radical removal. The reactions of RO_2 with NO generally possess terminating channels, forming the corresponding organic nitrate product, the branching ratios of which are sensitive to the size and structure of the RO_2 radical:

$$\mathrm{RO_2} + \mathrm{NO} \rightarrow \mathrm{RONO_2} \tag{11}$$

As indicated by the total nitrate product yields shown in Fig. 1, the average fraction of the RO_2 + NO reactions leading to first generation nitrate product formation in MCM v3.1 are assigned values of 24 and 25% for the oxidation of α- and β-pinene, respectively, based on the data reported by Ruppert et al. (1999) for a series of monoterpenes. The sensitivity to variations in the α-pinene nitrate yields, within the context of literature uncertainties, is discussed further below (Section 4.2).

The reactions with NO_2 tend to be most significant for acyl peroxy radicals, leading to the formation of peroxyacyl nitrates. The MCM v3.1 degradation schemes for α- and β-pinene include the respective formation of ca. 20 and ca. 30 acyl peroxy radicals (of generic formula $RC(O)O_2$). These include the acetyl peroxy radical, $CH_3C(O)O_2$, but are mainly complex multifunctional species, for example the (3-acetyl-2,2-dimethyl-cyclobutyl)-acetyl peroxy radical formed from the degradation of pinonaldehyde. The reversible reactions of

the $RC(O)O_2$ radicals with NO_2, to form the corresponding peroxyacyl nitrates, potentially leads to temporary loss of free radicals:

$$RC(O)O_2 + NO_2 \rightleftharpoons RC(O)OONO_2 \quad (12)$$

As described in detail elsewhere (Jenkin et al. 1997, 2003; Saunders et al. 2003), MCM v3.1 incorporates all the above types of process explicitly, in addition to competitive reactions which gain in significance at lower concentrations of NO_X.

The kinetics and mechanistic representation of the reactions of O_3 with α- and β-pinene is described in detail by Jenkin et al. (2000) and Saunders et al. (2003). In addition to supplementing the oxidation rate of the terpenes, these reactions have an important secondary influence through being sources of OH and other free radicals. The mechanism proceeds in each case via addition of O_3 to the double bond, leading initially to formation of energy rich ozonides. In the case of α-pinene (which contains an endocyclic double bond), the ozonide decomposes rapidly by two ring opening channels to form isomeric C_{10} carbonyl-substituted Criegee biradicals, which also possess excess energy. In the case of β-pinene (which contains an exocyclic double bond), the ozonide decomposes by two possible channels, forming either HCHO and an energy rich C_9 Criegee biradical, or nopinone and the energy rich Criegee biradical, $[CH_2OO]^*$. The energy rich Criegee biradicals are assumed to be either collisionally stabilized, or to decompose to yield OH and an additional organic radical. As described by Saunders et al. (2003), the representations in MCM v3.1, based in part on the structure-reactivity method proposed by Rickard et al. (1999), lead to overall fractional yields of OH (and the co-radicals) of 80 and 35%, respectively, which are consistent with the ranges reported in experimental studies: (68–91%) for α-pinene (Atkinson et al. 1992; Chew and Atkinson 1996; Paulson et al. 1998; Rickard et al. 1999; Siese et al. 2001; Aschmann et al. 2002b; Berndt et al. 2003); (24–35%) for β-pinene (Atkinson et al. 1992; Rickard et al. 1999). Sensitivity of the systems to uncertainties in the yields of OH (and the co-radicals) is discussed further below (Sections 4.2 and 4.3).

Although not normally of great significance in the atmosphere, the reactions of unsaturated organic compounds with $O(^3P)$, formed predominantly by photolysis of NO_2 (reaction (6)), can have a non-negligible impact under chamber conditions (e.g. Calvert et al. 2000). This is because of the concentrations of NO_X (and therefore NO_2) used in chamber studies tend to be greater than those typically observed in the atmosphere. As shown in Table 1, the NO_X concentrations in the experiments considered here lie in range of 0.1 to 1 ppm, whereas those in urban atmospheres are typically ≤0.1 ppm (e.g., Jenkin 2004, and references therein). The reactions with $O(^3P)$ can potentially influence the system in two ways, first by partially intercepting the formation of O_3 by reaction (7) and, secondly, by forming radical products and therefore influencing the radical balance in the system. The $O(^3P)$ initiation reactions were not considered in the construction of the MCM, and are therefore not represented in MCM v3.1. As part of the present study, reactions of $O(^3P)$ with α- and β-pinene, and associated chemistry, were incorporated into the mechanism, as summarised in Table 2. The rate coefficients are reasonably well determined, and were based on the recommendations of Calvert et al. (2000). The mechanisms and products of the reactions for alkenes in general have been reviewed and discussed in detail by Cvetanovic (1987) and Calvert et al. (2000). It is well established that the reaction proceeds mainly by addition to the double bond, forming a biradical adduct which can decompose, isomerise, or be collisionally stabilized to form an oxirane. There is some reported information on product channels, with the general indication that radical channels

Table 2 Product channels and branching ratios assigned to the reactions of $O(^3P)$ with α-pinene and β-pinene

Reaction	Branching ratio	Comment
$O(^3P)$ + α-pinene → α-pinene oxide	0.77	(a)
→ 2,6,6-trimethyl-bicyclo[3.1.1]heptan-3-one	0.23	(a)
$O(^3P)$ + β-pinene → β-pinene oxide	0.77	(b)
→ 6,6-dimethyl-bicyclo[3.1.1]heptane-2-carbaldehyde	0.23	(b)

(a) $k = 3.2 \times 10^{-11}$ cm^3 molecule^{-1} s^{-1}, based on the recommendation of Calvert et al. (2000). Branching ratios are based on the results of Alvarado et al. (1998), who observed the formation of α-pinene oxide and two carbonyl products isomeric with α-pinene oxide. The carbonyl products are represented by the displayed species, which is already formed from α-pinene degradation in MCM v3.1, appearing as APINBCO. α-pinene oxide removed by reaction with OH (estimated $k = 1.2 \times 10^{-11}$ cm^3 molecule^{-1} s^{-1}) to form products already present in mechanism.

(b) $k = 2.7 \times 10^{-11}$ cm^3 molecule^{-1} s^{-1}, based on the recommendation of Calvert et al. (2000). Branching ratios are inferred from the results of Alvarado et al. (1998) for α-pinene (see note (a)). The displayed carbonyl product is isomeric with β-pinene oxide, and is already formed from β-pinene oxide degradation in MCM v3.1, appearing as C918CHO. β-pinene oxide removed by reaction with OH (estimated $k = 1.2 \times 10^{-11}$ cm^3 molecule^{-1} s^{-1}) to form products already present in mechanism.

dominate for smaller alkenes, with the formation of molecular products becoming progressively more important for larger alkenes (e.g. Calvert et al. 2000). Accordingly, Alvarado et al. (1998) observed exclusive formation of molecular products from the reaction of $O(^3P)$ with α-pinene, with dominant formation of the oxirane product, α-pinene oxide. As shown in Table 2, the results of Alvarado et al. (1998) form the basis of the treatment adopted in the present study for the reaction of $O(^3P)$ with α-pinene. In the absence of experimental studies, the products and branching ratios for the reaction of $O(^3P)$ with β-pinene are inferred by analogy with those of α-pinene.

4 Mechanism evaluation

In the present evaluation, as with previous assessments (e.g. Carter 2000; Pinho et al. 2005, 2006), the quantity $D(O_3–NO)$ was used as the main criterion of model performance. This quantity is defined as: $D(O_3 - NO)_t = [O_3]_t - [NO]_t - \left([O_3]_0 - [NO]_0\right)$, where $[O_3]_0$, $[NO]_0$, and $[O_3]_t$, $[NO]_t$ are the concentrations of O_3 and NO at the beginning of the run, and at time 't,' respectively. As described in detail previously (e.g., Carter and Lurmann 1991; Carter et al. 1995a; Carter 2000), $D(O_3–NO)$ is an indicator of the ability of the mechanism to simulate the chemical processes that cause O_3 formation, giving a useful measure of reaction development, even when O_3 is suppressed by the presence of excess NO. The precursor decay rate and the formation of carbonyl products were also used as criteria of model performance, whenever the experimental information exists.

In the current evaluation the designation 'MCM v3.1' includes the parameter updates described by Pinho et al. (2005), based on evaluation of isoprene and butane degradation. Most of these have negligible or zero impacts on the present evaluation, because they relate to reactions of species not generated from degradation of the terpenes considered here. However, the implementation of revised photolysis parameters for HCHO is of significance, leading to a ca. 10% increase in radical formation from HCHO photolysis and slightly more efficient ozone formation.

The performance of the α- and β-pinene mechanisms, and sensitivity to a number of parameter and mechanistic variations, are described in the following subsections. In addition,

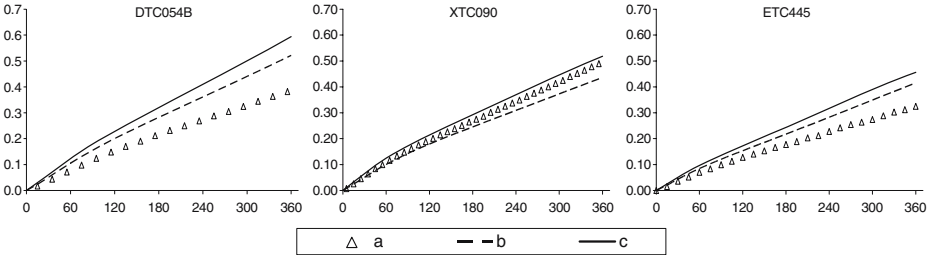

Fig. 2 Example plots of experimental and calculated D(O_3–NO) (ppm) vs. time (min) for the acetone-NO_X -air experiments: **a** experimental data; **b** MCM v3.1; **c** MCM v3.1 with the upgrade in photolysis data. DTC054B- acetone/NO_X=38.3; XTC090- acetone/NO_X=49.6; ETC445- acetone/NO_X=61.9

the performance of the mechanism for the degradation product acetone is also evaluated. Because of space limitations, comparisons of simulated and observed quantities are illustrated for only a subset of the experiments considered. Where possible, the three presented examples in each case are an experiment at the low end of the [VOC]/[NO_X] range, and experiment at intermediate [VOC]/[NO_X] and an experiment at the high end of the [VOC]/[NO_X] range. The full set of comparisons is available on request from the authors.

4.1 Acetone/NO_X experiments

The simulated D(O_3–NO) and HCHO formation rates, and acetone loss rates were found to be well described for the series of acetone-NO_X photo-oxidation experiments, using MCM v3.1 (see Figs. 2, 3 and 4). For consistency with our previous evaluations (Pinho et al. 2005), the opportunity was taken to revise the photolysis parameters for acetone in line with the latest recommendation of the IUPAC panel (Atkinson et al. 2006). As described by Jenkin et al. (1997), those in MCM v3.1 were previously based on the absorption cross-sections of Martinez et al. (1992) and the quantum yields of Meyrahn et al. (1986). The revised absorption cross sections are based on the measurements of Gierczak et al. (1998), which agree well with those reported by Martinez et al. (1992) at room temperature. The revised quantum yields are based on the appraisal of Warneck (2001), and are greater than those reported by Meyrahn et al. (1986) by ca. 40% on average over the wavelength range 280–320 nm at room temperature and 1 bar. Consequently, the revision leads to increased radical formation by reaction (9), and slightly increased D(O_3–NO) and HCHO formation rates, and acetone loss rates (see Figs. 2, 3 and 4), although these are still in acceptable

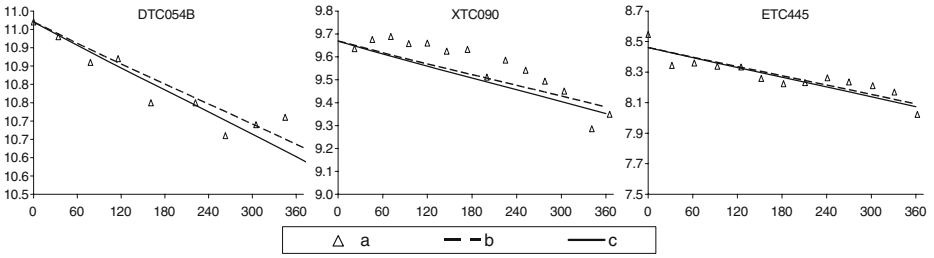

Fig. 3 Example plots of experimental and calculated acetone (ppm) vs. time (min) for the acetone-NO_X -air experiments: **a** experimental data; **b** MCM v3.1; **c** MCM v3.1 with the upgrade in photolysis data. DTC054B- acetone/NO_X=38.3; XTC090- acetone/NO_X=49.6; ETC445- acetone/NO_X=61.9

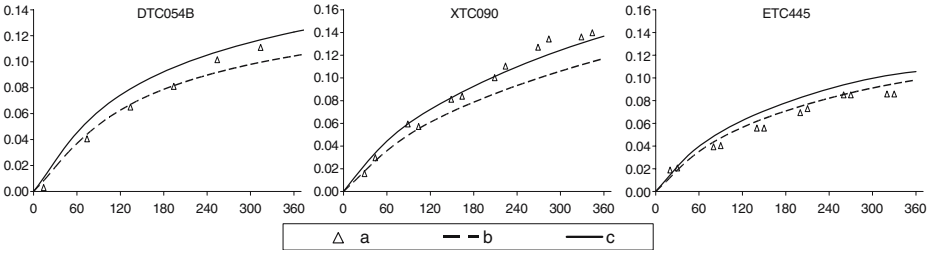

Fig. 4 Example plots of experimental and calculated HCHO (ppm) vs. time (min) for the acetone-NO_X -air experiments: **a** experimental data; **b** MCM v3.1; **c** MCM v3.1 with the upgrade in photolysis data. DTC054B- acetone/NO_X=38.3; XTC090- acetone/NO_X=49.6; ETC445- acetone/NO_X=61.9

agreement with the experimental results. It is also apparent from the figures that the loss rate of acetone is very slow (typically ca. 4% in 6 h), by virtue of its low OH reactivity and photolysis rate, with notable formation of D(O_3–NO) and HCHO resulting from the very

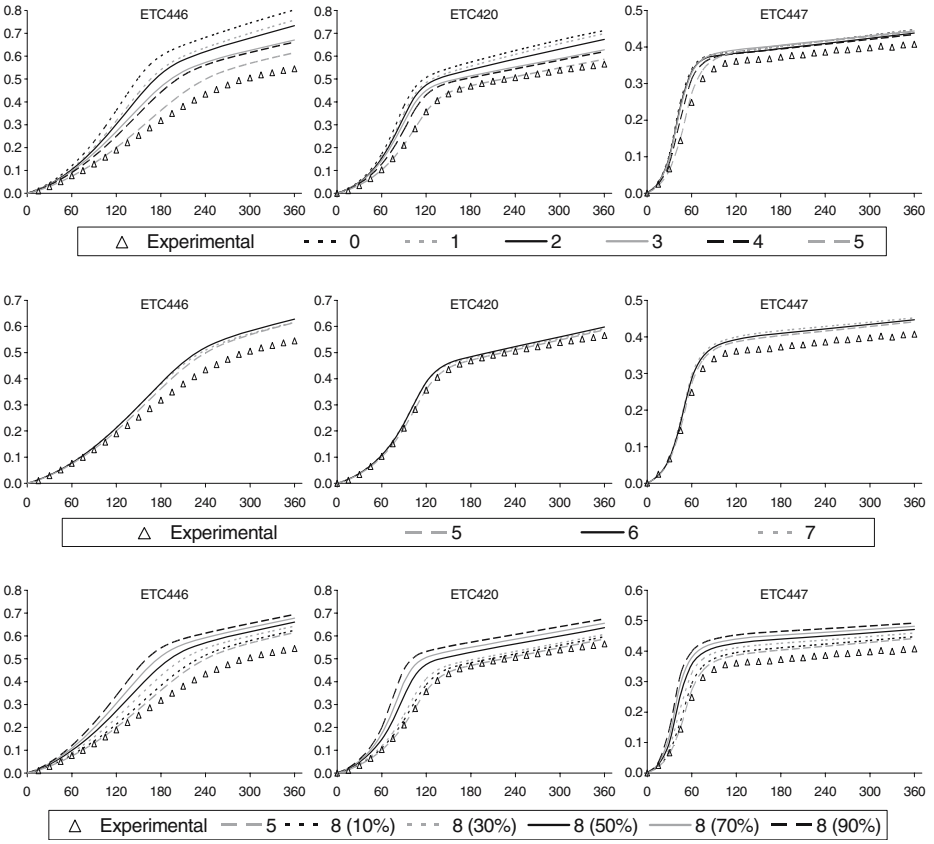

Fig. 5 Example plots of experimental and calculated D(O_3–NO) (ppm) vs. time (min) for the α-pinene-NO_X -air experiments. ETC446-α-pinene/NO_X=0,508; ETC420-α-pinene/NO_X=0.906; ETC447-α-pinene/NO_X=2.058. Legend: *numbers* correspond to mechanistic variations tested, see Table 3. For mechanism 8, the *numbers inside brackets* correspond to percentage of isomerisation of APINAO

high mixing ratios of acetone employed. In the terpene systems, therefore, the further oxidation of product acetone is negligible on the timescale of chamber experiments and cannot contribute significantly to ozone formation.

4.2 α-pinene/NO_X experiments

The D(O_3–NO) formation rate and α-pinene loss rate, simulated using MCM v3.1, were generally found to overestimate the experimental observations (see Figs. 5 and 6, Mechanism 0), with the average simulated D(O_3–NO) being 27% greater than observation, based on the complete series of experiments. The average extent of over-simulation increases with decreasing initial VOC/NO_X, varying from 11% in the highest VOC/NO_X experiment (ETC447: VOC/NO_X=2.128) to 60% in the lowest VOC/NO_X experiment (ETC446: VOC/NO_X=0.523) (see Fig. 7). This result is therefore consistent with the previous analysis of EUPHORE data (Saunders et al. 2003), which showed that the MCM was able to recreate the results of three experiments carried out at much higher initial VOC/NO_X than considered here (i.e., 3.0, 9.2 and ∞). The influence of incorporating the $O(^3P)$

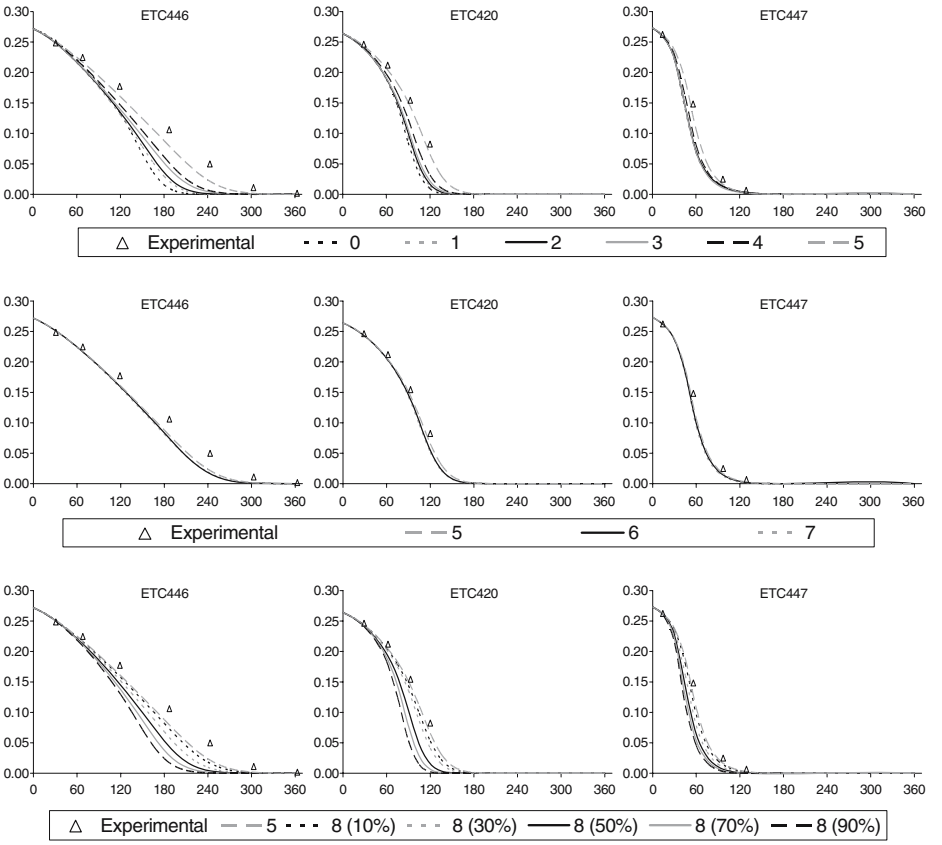

Fig. 6 Example plots of experimental and calculated α-pinene (ppm) vs. time (min) for the α-pinene-NO_X -air experiments. ETC446-α-pinene/NO_X=0,508; ETC420-α-pinene/NO_X=0.906; ETC447-α-pinene/NO_X=2.058. Legend: *numbers* correspond to mechanistic variations tested, see Table 3. For mechanism 8, the *numbers inside brackets* correspond to percentage of isomerisation of APINAO

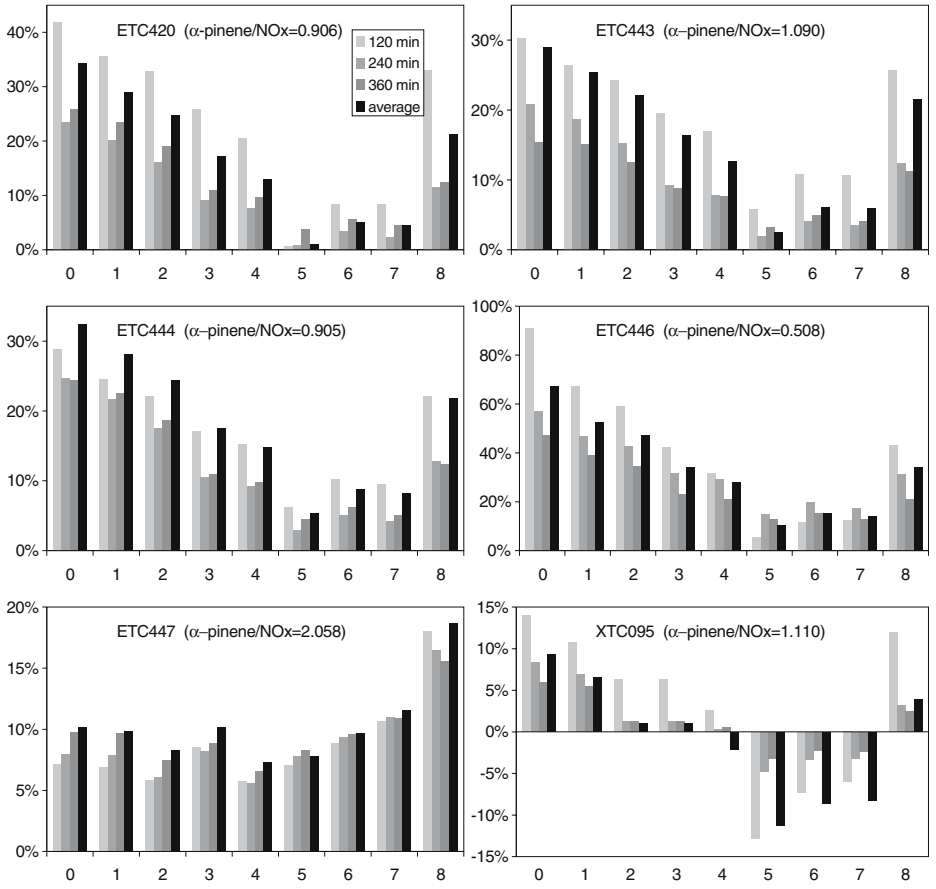

Fig. 7 Deviation of simulated D(O_3–NO) from experimental observations in the six α-pinene/NO_X photo-oxidation experiments for the mechanistic variants listed in Table 3 and described in the text. The comparison is shown for the average and three time points in each experiment, with the deviation defined as (calc-obs)/obs. For mechanism 8, the example presented is for 50% 1,5-H shift isomerisation of APINAO (see text and Fig. 5)

initiated chemistry into the MCM v3.1 α-pinene mechanism was investigated, using the reaction pathways and subsequent chemistry summarised in Table 2. As shown in Figs. 5, 6 and 7 (Mechanism 1), this slightly reduced the simulated rates of D(O_3–NO) formation and α-pinene decay, with the effect once again being more discernable at low VOC/NO_X (the average over-simulation of D(O_3–NO) was reduced to 22%). The general overestimation in the simulated quantities may be indicative of systematic errors in the input of radicals to the system (i.e. overestimated sources and/or underestimated sinks), or in ozone formation chain lengths of portions of the mechanism under NO_X-rich conditions, or both. Sensitivity of the system to a number of parameter uncertainties and proposed mechanistic variations reported in the literature was therefore tested, as listed in Table 3. As described in the following subsections, the collective implementation of a number of refinements allows the D(O_3–NO) and α-pinene simulations to be brought into good agreement with the experimental observations, with each of the refinements being consistent with reported parameter uncertainty ranges or mechanistic adjustments (Mechanisms 2–5). The additional simulations

Table 3 Summary of mechanistic variations tested for the α-pinene/NO_X photo-oxidation experiments

Mechanism number	Description
0	MCM v3.1
1	MCM v3.1 with $O(^3P)$ + α-pinene reaction included
2	Mechanism 1 with revised photolysis channels for pinonaldehyde, norpinonaldehyde and hydroxypinonaldehydes
3	Mechanism 2 with revised degradation chemistry for pinonldehyde and some related species
4	Mechanism 3 with yield of nitrates formed in initial OH-initiated, NO-catalysed degradation chemistry increased from 24% to 27%
5	Mechanism 4 with yield of OH (and co-radical) from O_3 + α-pinene decreased from 80% to 70%
6	Mechanism 5 with some reported variations to radical propagation pathways to first generation products: (a) modified branching ratios for OH attack on α-pinene; (b) competing ring closure of peroxy radical APINCO2.
7	Mechanism 5 with formation of HCHO as a first generation product following competing CH_3 radical ejection from oxy radical APINAO.
8	Mechanism 5 with formation of HCHO as a first-generation product, following competing 1,5-H atom shift isomerisation of oxy radical APINAO

using Mechanisms 6–8 explore the sensitivity of the system to several other reported mechanistic variations which potentially impact on the first generation product distribution and the ozone formation chain length of the initial oxidation step.

4.2.1 Degradation of pinonaldehyde and related products

The photolysis of pinonaldehyde and related species in MCM v3.1 is assumed to generate radical products exclusively (see Section 3). Although the applied photolysis rate is consistent with the observed removal rate of pinonaldehyde in the EUPHORE chamber (RADICAL 2002), a number of studies have demonstrated a progressive increase in the importance of molecular product channels with carbon number for a series of C_4–C_7 aldehydes (Tadic et al. 2001a,b, 2002; RADICAL 2002), which implies probable dominant formation of molecular products from pinonaldehyde photolysis for the relevant range of wavelengths. Based on the molecular contribution of 80% reported for the photolysis of heptanal (Tadic et al. 2002), the largest aldehyde studied, and notionally allowing for the much smaller contribution to radical formation from photolysis of the ketone group in pinonaldehyde (which is not explicitly represented), we assign revised contributions of 76 and 24% to molecular and radical channels, respectively, which are also similar to those applied in the theoretical study of Capouet et al. (2004). The radical-forming channel proceeds via the Norrish "Type I" process (reaction 10), with the molecular channel forming methylvinyl ketone and a C_6 unsaturated aldehyde (reaction 13), where R′ represents the 3-acetyl-2,2-dimethyl-cyclobutyl group:

$$R'CH_2CHO + h\upsilon \rightarrow CH_3C(O)CH=CH_2 + CH_3C(CH_3)=CHCH_2CHO \qquad (13)$$

For consistency, the photolysis channels for the related species norpinonaldehyde and three hydropinonaldehyde isomers, formed in the MCM α-pinene degradation scheme, were treated analogously. As shown in Figs. 5, 6 and 7 (Mechanism 2) the reduced radical

production resulting from these changes leads to a reduction in D(O_3–NO) formation and α-pinene loss in the latter stages of the simulations when pinonaldehyde (and related species) have accumulated to significant concentrations, with the average over-simulation of D(O_3–NO) being reduced to 19%, based on the complete series of experiments. The majority of the impact results from the implementation of the revised product channel ratios for pinonaldehyde itself, with the changes for the related species having a smaller additional effect.

The OH-initiated degradation of pinonaldehyde in MCM v3.1 is assumed to proceed via two H-abstraction channels, accounting for ca. 77 and 23% of the reaction, respectively,

$$OH + R'CH_2CHO(+O_2) \rightarrow R'CH_2C(O)O_2 + H_2O \quad (14)$$

$$OH + R'CH_2CHO(+O_2) \rightarrow R'_{-H}(O_2)CH_2CHO + H_2O \quad (15)$$

where $R'_{-H}(O_2)CH_2CHO$ represents the tertiary peroxy radical formed following attack on the cyclobutyl ring at the position β to the aldehyde group. Fantechi et al. (2002) have carried out a detailed theoretical appraisal on the OH initiated degradation of pinonaldehyde, considering attack at six positions and the subsequent chemistry. Of these, the three most important routes were calculated to account for 90.5% of the reaction, including reactions (14) and (15) with probabilities of 59 and 8.5%. A further significant channel, accounting for 23% of the reaction, was identified:

$$OH + R'CH_2CHO(+O_2) \rightarrow R'CH(O_2)CHO + H_2O \quad (16)$$

Whereas reactions (14) and (15) initiate NO_X-catalysed propagation sequences involving several NO-to-NO_2 conversions, reaction (16) leads to a comparatively short sequence, yielding norpinonaldehyde (R′CHO) and CO, and is thus less efficient at generating ozone:

$$R'CH(O_2)CHO + NO \rightarrow R'CH(O)CHO + NO_2 \quad (17)$$

$$R'CH(O)CHO + NO \rightarrow R'CHO + HCO \quad (18)$$

$$HCO + O_2 \rightarrow CO + HO_2 \quad (19)$$

This reaction sequence (and associated competing reactions for the $R'CH(O_2)CHO$ intermediate) was therefore implemented, and the relative contributions of the three reaction channels (14–16) were set to be consistent with those determined by Fantechi et al. (2002), but scaled to account for the entire reaction, i.e. 65.2, 9.4 and 25.4% for channels (14), (15) and (16), respectively. In addition, analogous channels were incorporated for the OH-initiated degradation of the hydroxypinonaldehydes. As shown in Figs. 5, 6 and 7 (Mechanism 3) the reduced ozone formation chain lengths resulting from these changes leads to a notable reduction in D(O_3–NO) formation and α-pinene loss in the latter stages of the simulations when the pinonaldehyde (and related species) have accumulated to significant concentrations, with the average over-simulation of D(O_3–NO) being further reduced to 14%, based on the complete series of experiments. Once again, the majority of the impact results from the implementation of the revised chemistry for pinonaldehyde itself.

4.2.2 Radical removal from the reactions of RO_2 with NO in the initial oxidation sequence

As described in Section 3 and Fig. 1, the total nitrate yield in the primary oxidation sequence for α-pinene is based on the FTIR product study of Ruppert et al. (1999). A value of 24% was reported in that study, with an inferred error limit of ca. ±1.3%, based on the quoted uncertainty in the integrated nitrate band absorption cross section used to quantify the yield. A further determination was made subsequently by Nozière et al. (1999), who reported a value of (18±9%) using the same method. The impact of increasing the nitrate yield to the high end of the reported uncertainty range (27%) was therefore tested, thereby increasing radical termination via reaction type (11) in the initial OH-initiated oxidation step. As shown in Figs. 5, 6 and 7 (Mechanism 4) this reduces the rate of D(O_3–NO) formation and α-pinene loss in the early stages of the experiment, with the average over-simulation of D (O_3–NO) being further reduced to 11%, based on the complete series of experiments. It is noted that Aschmann et al. (2002a) have more recently reported a very low nitrate yield of ca. 1%, determined using atmospheric pressure ionisation mass spectrometry which, as indicated by Aschmann et al. (2002a), is difficult to reconcile with the reported ranges and trends in nitrate yields from the reactions of alkyl and hydroxyalkyl peroxy radicals with NO in general (e.g., O'Brien et al. 1998; Aschmann et al. 2001). Clearly, the use of this value in the present simulations would substantially reduce radical termination in the system, and similarly increase the D(O_3–NO) formation and α-pinene loss rates.

4.2.3 Radical formation from the ozonolysis of α-pinene

The yield of OH, and its co-radical(s), from the ozonolysis of α-pinene is reported to lie in the range 68–91%, with the mechanistic representation used in MCM v3.1 leading to a yield of 80% (see Section 3). Owing to the previously demonstrated sensitivity of alkene-NO_X photo-oxidation simulations to ozonolysis radical yields (Pinho et al. 2006), the effect of a modest reduction in the yield of OH, and its co-radical(s), to close to the low end of the reported range (70%) was investigated. As shown in Figs. 5, 6 and 7 (Mechanism 5) this has a significant reducing impact on the level of D(O_3–NO) throughout most of the experiments, and a corresponding effect on the rate of α-pinene loss. The cumulative effect of all the mechanism and parameter variations described above, is therefore to reduce the simulated average D(O_3–NO) from an overestimate of 26% using MCM v3.1 to a value of 3% (range +10.8% to −12.0%), with the resultant representation providing an acceptable description of the chamber dataset.

4.2.4 Variations in radical propagation pathways to first generation products

A number of studies by Peeters and co-workers (Peeters et al. 2001; Vereecken and Peeters 2004; Capouet et al. 2004) have considered the relative importance of the various pathways involved in the OH-initiated oxidation of α-pinene to first generation products. Although these studies have confirmed some aspects of the representation used in MCM v3.1, they have also recommended a substantially different initial OH attack distribution and have identified a number of alternative reactions for intermediate peroxy and oxy radicals. The sensitivities of the present chamber simulations to these processes were therefore investigated. The calculations of Peeters et al. (2001) confirmed that the initiation reaction is dominated by addition of OH to the double bond, but determined an associated peroxy radical distribution of (0.25: 0.50: 0.25) for APINAO2: APINBO2: APINCO2. Initial implementation of these branching ratios was found to lead to a small increase in D(O_3–NO)

formation in all experiments. This is a consequence of the increased importance of the APINCO2 channel (from 7.5 to 25%), the propagation chemistry of which contains one additional NO-to-NO_2 conversion than the other pathways, and which produces first generation products of higher average reactivity, by virtue of formation of the highly reactive unsaturated hydroxycycloketone product. Vereecken and Peeters (2004) also calculated that APINCO2 potentially undergoes a ring closure reaction, via internal addition to the double bond. This was estimated to occur with a rate constant of 2.5 s^{-1}, indicating that it is favoured over reaction with NO at mixing ratios below about 10–15 ppb NO. Although the ring closure reaction cannot compete at the initial levels of NO in the chamber experiments considered here, the NO mixing ratio decays rapidly during each experiment such that approximately half of the α-pinene is typically oxidised under conditions where the ring closure reaction is calculated to be major fate of APINCO2. This process was therefore also implemented, based on the representation presented in Capouet et al. 2004, with the following main propagation sequence:

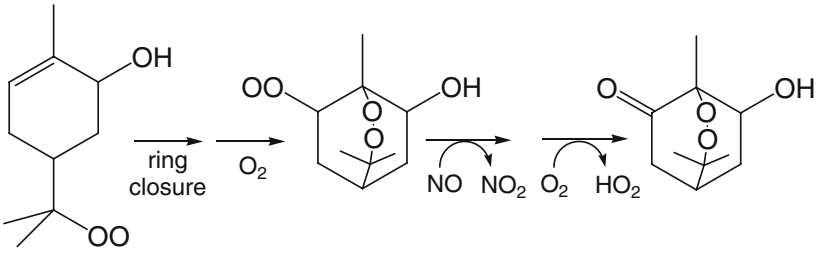

(20)

Associated reactions of the cyclic peroxy radical were also represented, and the cycloketone product was degraded to generate appropriate species already present in the mechanism. As shown in Figs. 5, 6 and 7 (Mechanism 6) inclusion of the modified initiation branching ratios and the ring closure reaction was found to have a small increasing effect on D(O_3–NO) formation and α-pinene removal. This results almost entirely from the modified initiation branching ratios (as discussed above), with implementation of the ring-closure reaction for APINCO2 having a very subtle reducing (i.e., compensating) effect in the latter stages of the simulation. This is a consequence of the associated propagation sequence having one fewer NO-to-NO_2 conversions than the pathway involving the APINCO2 + NO reaction, and because the associated first generation product reactivity is lower by virtue of loss of the double bond.

Capouet et al. (2004) also investigated the final step in the formation of pinonldehyde as a first generation product, which involves the reaction of either of two isomeric C_{10} α-hydroxy organic radicals with O_2, with the α-hydroxy organic radicals being formed from the ring opening of APINAO and APINBO. The mechanism of this class of reaction is generally accepted to involve the isomerisation and decomposition of an energy rich α-hydroxyperoxy radical intermediate, e.g. for radicals possessing an α-hydrogen:

$$\mathrm{RCHOH} + \mathrm{O_2} \rightarrow [\mathrm{RCH(OH)O_2}]^{\ddagger} \rightarrow \mathrm{RCHO} + \mathrm{HO_2} \tag{21}$$

However, the observed formation of HCOOH from the OH-initiated oxidation of α-pinene (Orlando et al. 2000) and cyclohexa-1,3-diene (Jenkin et al. 2005) in the presence of NO, has been interpreted in terms of the significant formation of stabilised α-hydroxyperoxy radical intermediates, $RCH(OH)O_2$, as the size of the organic group increases. The much slower decomposition rate of the stabilised $RCH(OH)O_2$ allows reaction with NO to

compete under the conditions employed in those studies, allowing HCOOH formation by reaction sequence (23) and (24) for radicals possessing an α-hydrogen,

$$RCH(OH)O_2 \rightarrow RCHO + HO_2 \quad (22)$$

$$RCH(OH)O_2 + NO \rightarrow RCH(OH)O + NO_2 \quad (23)$$

$$RCH(OH)O \rightarrow HCOOH + R \quad (24)$$

with the possibility of higher acids (R′C(=O)OH) being formed from the fully alkyl-substituted α-hydroxyperoxyradicals of generic formula $RCR'(OH)O_2$. Based partially on theoretical estimates of the rates of the processes involved, Capouet et al. (2004) determined that stabilisation of the energy-rich C_{10} α-hydroxyperoxy radicals generated from α-pinene dominates over decomposition, with the decomposition of the stabilised radicals estimated to occur at rates of $k_{25} = 1.25 \times 10^3\ s^{-1}$ and $k_{26} = 1.9 \times 10^4\ s^{-1}$:

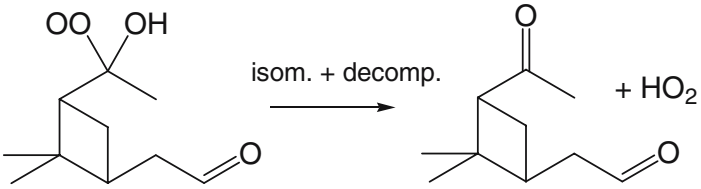

(25)

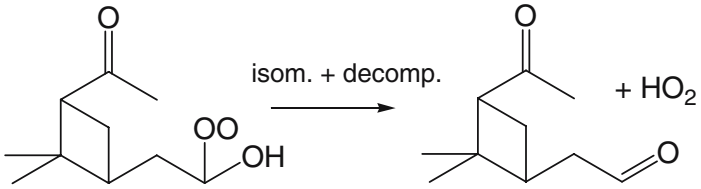

(26)

For completeness, this chemistry was also incorporated explicitly into the current mechanistic evaluation, although it was recognised that even a mixing ratio of 1 ppm NO would only allow small fractions of the stabilised α-hydroxyperoxy radicals to react with NO, i.e. about 15 and 1% compared with reactions (25) and (26), respectively. Accordingly, the results confirmed that this chemistry has a negligible effect for the conditions of the present chamber experiments, and more generally for α-pinene oxidation in the atmosphere. As pointed out by Capouet et al. (2004), however, it may have a greater impact at the higher NO concentrations employed in some published product studies of the OH-initiated oxidation of α-pinene, and may therefore be a contributory factor in accounting for the range of pinonaldehyde yields reported (see Section 3).

4.2.5 Pathways forming formaldehyde

The modifications implemented in Mechanism 5 allow a good description of the $D(O_3–NO)$ and α-pinene profiles, but the mechanism generally underestimates the formation of HCHO by a factor of about two (see Fig. 8). As described in Section 3 and Fig. 1, MCM v3.1 (and the mechanistic variants described above) does not include any routes which yield HCHO

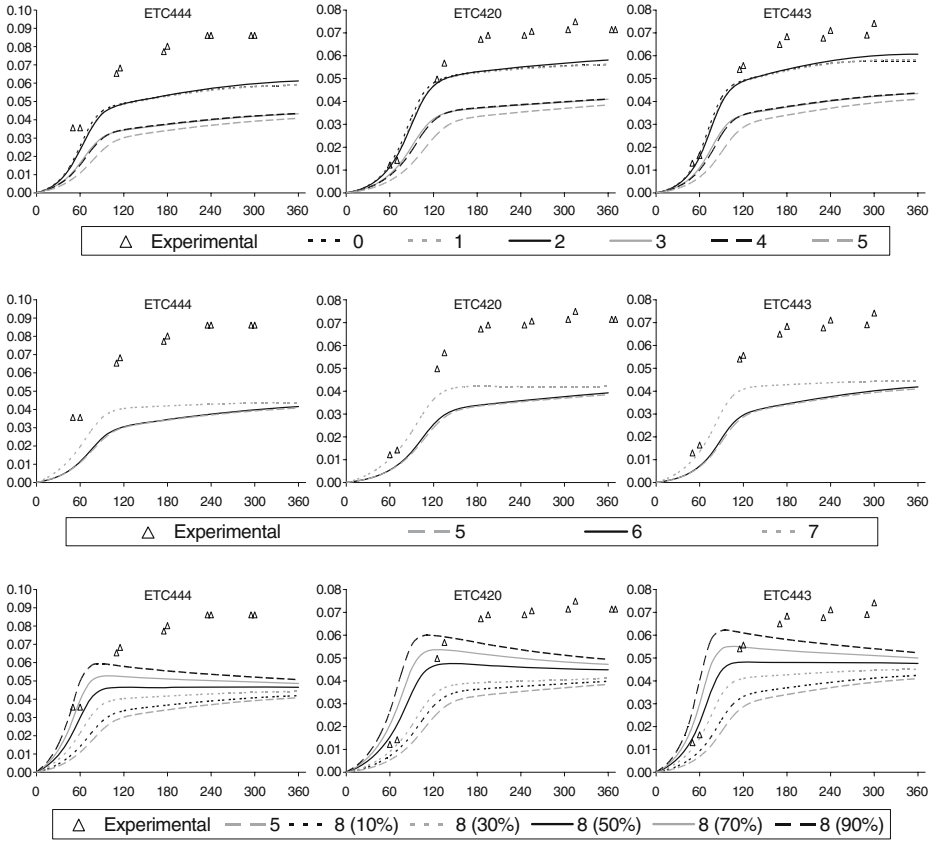

Fig. 8 Example plots of experimental and calculated HCHO (ppm) vs. time (min) for the α-pinene-NO_X-air experiments. ETC444-α-pinene/NO_X=0.905; ETC420-α-pinene/NO_X=0.906; ETC444-α-pinene/NO_X=1.09. Legend: *numbers* correspond to mechanistic variations tested, see Table 3. For mechanism 8, the *numbers inside brackets* correspond to percentage of isomerisation of APINAO

as a first generation product. Furthermore, the modifications to pinonaldehyde degradation described and justified above, also reduce formation of HCHO as a second generation product by virtue of the increased formation of norpinonaldehyde via the shorter oxidation sequence, reactions (16–18). The effects of implementing postulated routes to the formation of HCHO as a first generation product were therefore examined.

The decomposition of APINAO by ejection of CH_3 was implemented into Mechanism 5, such that it accounted for 31% of the fate of the radical, as postulated by Nozière et al. (1999):

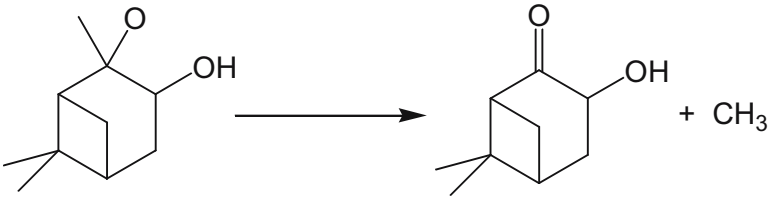

(27)

The further oxidation of CH_3, following initial formation of CH_3O_2, yields HCHO primarily by the well-established sequence involving one additional NO-to-NO_2 conversion:

$$CH_3O_2 + NO \rightarrow CH_3O + NO_2 \quad (28)$$

$$CH_3O + O_2 \rightarrow HCHO + HO_2 \quad (29)$$

The 3-hydroxynopinone co-product of reaction (27) is also generated from β-pinene degradation, and was therefore degraded according to the MCM v3.1 representation. As shown in Fig. 8 (Mechanism 7), incorporation of this chemistry generally improves the simulation of HCHO, although the final yields are still significantly underestimated. However, part of this improvement is a consequence of a general increase in the extent of chemical processing, as indicated by the increased formation rate of D(O_3–NO) and decay rate of α-pinene (Figs. 5, 6 and 7), which results from the additional NO-to-NO_2 conversion by reaction (28) and the increased secondary radical production via HCHO photolysis.

The potential role of a competing 1,5-H atom shift isomerisation reaction for APINAO was also considered, to examine the impact of this and similar reactions as postulated by Aschmann et al. (1998), Orlando et al. (2000) and Davis and Stevens (2005). The following main propagation sequence was represented, producing HCHO:

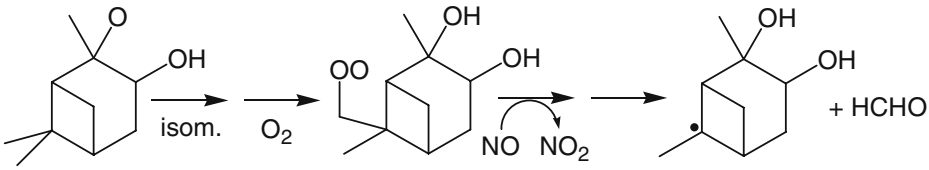

(30)

This contains one additional NO-to-NO_2 conversion, with the further reaction sequence of the C_9 dihydroxy radical product possessing a further two NO-to-NO_2 conversions prior to formation of a stable dihydroxydiketone product and HO_2. As shown in Fig. 8 (Mechanism 8), increasing the importance of the isomerisation reaction substantially increases the formation of HCHO. However, once again there is a corresponding progressive increase in the extent of chemical processing (see Figs. 5, 6 and 7), which is even more enhanced in this case because of the three additional NO-to-NO_2 conversions accompanying the HCHO formation mechanism. The simulated formation rate of D(O_3–NO) and decay rate of α-pinene therefore also increase substantially, leading to a poor comparison with the experimental data. As a result, it is not possible to match the shape of the observed HCHO profile by increasing the importance of this route to its first generation production.

Peeters et al. (2001) also considered the possible participation of the above decomposition and isomerisation routes for APINAO in their theoretical appraisal of the OH-initiated oxidation of α-pinene. They calculated that decomposition via reaction (27) is uncompetitive and that the 1,5-H atom migration step which initiates reaction sequence (30) accounts for ≤12.5% of the fate of APINAO, the dominant fate being ring opening, as represented in MCM v3.1 and the mechanistic variants described above. It should also be noted that the MCM pinonaldehyde degradation chemistry (both before and after the modifications described above) and the theoretical appraisals/simulations of pinonaldehyde

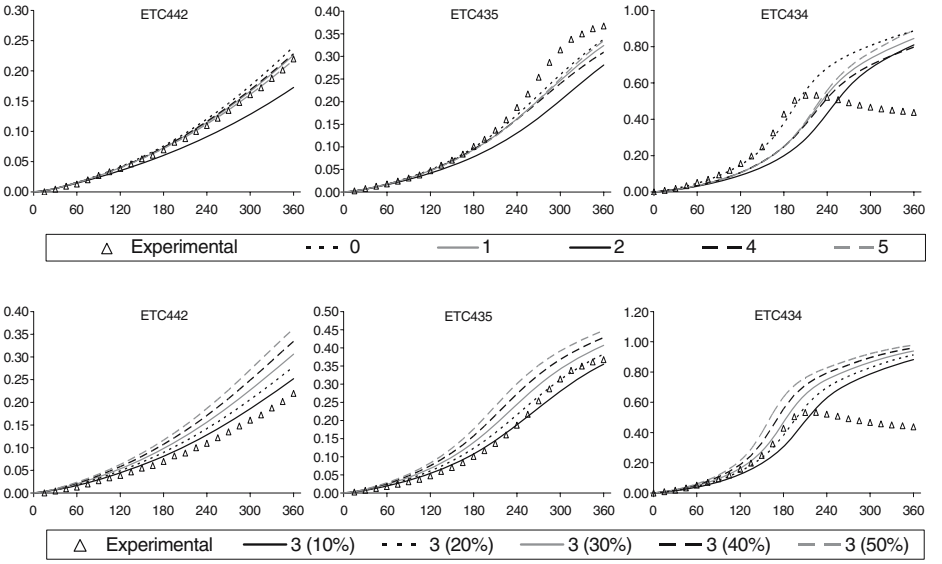

Fig. 9 Example plots of experimental and calculated $D(O_3–NO)$ (ppm) vs. time (min) for the β-pinene-NO_X-air experiments. ETC442-β-pinene/NO_X=0.946; ETC435-β-pinene/NO_X=2.018; ETC434-β-pinene/NO_X=3.301. Legend: *numbers* correspond to mechanistic variations tested, see Table 4. For mechanism 3, the *numbers inside brackets* correspond to percentage of isomerisation of BPINAO

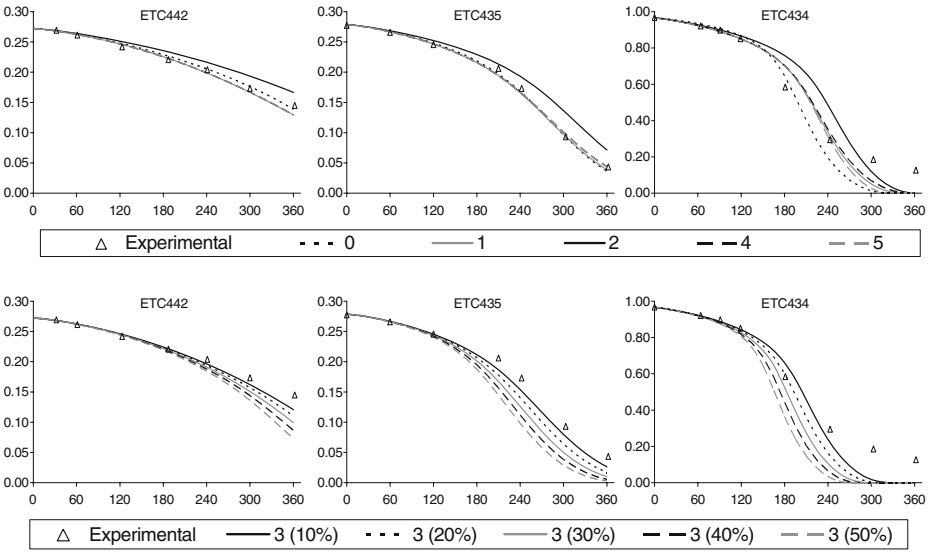

Fig. 10 Example plots of experimental and calculated β-pinene (ppm) vs. time (min) for the β-pinene-NO_X-air experiments. ETC442-β-pinene/NO_X=0.946; ETC435-β-pinene/NO_X=2.018; ETC434-β-pinene/NO_X=3.301. Legend: *numbers* correspond to mechanistic variations tested, see Table 4. For mechanism 3, the *numbers inside brackets* correspond to percentage of isomerisation of BPINAO

degradation of Fantechi et al. (2002) and Capouet et al. (2004) cannot be reconciled with the high HCHO molar yield (ca. 150%) reported by Nozière et al. (1999).

4.3 β-pinene/NO_X experiments

The D(O_3–NO) formation rate and β-pinene loss rate, simulated using MCM v3.1, were broadly comparable with the experimental observations (see Figs. 9, 10 and 11, Mechanism 0), but with a tendency to overestimation at low VOC/NO_X. The influence of incorporating the $O(^3P)$ initiated chemistry into the MCM v3.1 β-pinene mechanism was investigated, using the reaction pathways and subsequent chemistry summarised in Table 2. As shown in Figs. 9, 10 and 11 (Mechanism 1), this reduced the simulated rates of D(O_3–NO) formation and β-pinene decay in all experiments, leading to an improvement in agreement at low VOC/NO_X, but a tendency towards underestimation at the high end of the VOC/NO_X range. As shown in Fig. 9,

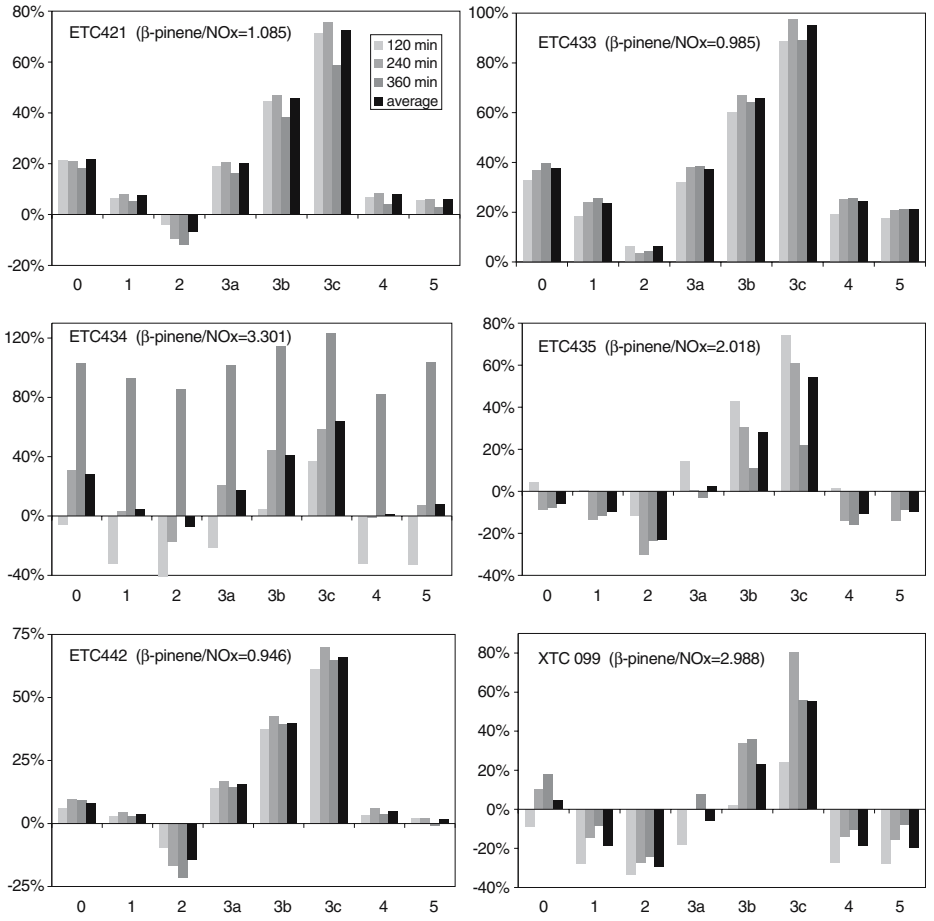

Fig. 11 Deviation of simulated D(O_3–NO) from experimental observations in the six β-pinene/NO_X photo-oxidation experiments for the mechanistic variants listed in Table 4 and described in the text. The comparison is shown for the average and three time points in each experiment, with the deviation defined as (calc-obs)/obs. For mechanism 3, the examples presented (3a, 3b and 3c) are for 10, 30 and 50% 1,5-H shift isomerisation of BPINAO, respectively (see text and Fig. 9)

Table 4 Summary of mechanistic variations tested for the β-pinene/NO_X photo-oxidation experiments

Mechanism number	Description
0	MCM v3.1
1	MCM v3.1 with $O(^3P)$ + β-pinene reaction included
2	Mechanism 1 with some reported variations to radical propagation pathways to first generation products: (a) modified branching ratios for OH attack on β-pinene; (b) competing ring closure of peroxy radical BPINCO2
3	Mechanism 1 with formation of HCHO, following competing 1,5-H atom shift isomerisation of oxy radical BPINAO
4	Mechanism 1 with modified branching ratios for OH attack on nopinone
5	Mechanism 1 with modified branching ratios for OH attack on nopinone. OH attack assumed to proceed entirely via the 4-nopinonyl route, and with 4-nopinonoxy radical artificially assumed to react exclusively with O_2

it was also not possible to recreate the observed cessation of chemical processing after ca. 200 min in the highest VOC/NO_X experiment (ETC434) because, in contrast to the observations, very small (i.e. non-zero) levels of NO were simulated to persist to the end of the experiment, allowing ozone formation to continue under the prevailing NO_X-limited conditions. The observed phenomenon could only be achieved by inclusion of an efficient artificial sink for NO_X becoming active at the appropriate point. The simulations of HCHO and nopinone (which are both formed as major first generation products) show broadly the same level of agreement with observations (Figs. 12 and 13) as displayed by D(O_3–NO) in the series of experiments, although nopinone levels tended to display a greater extent of over-simulation

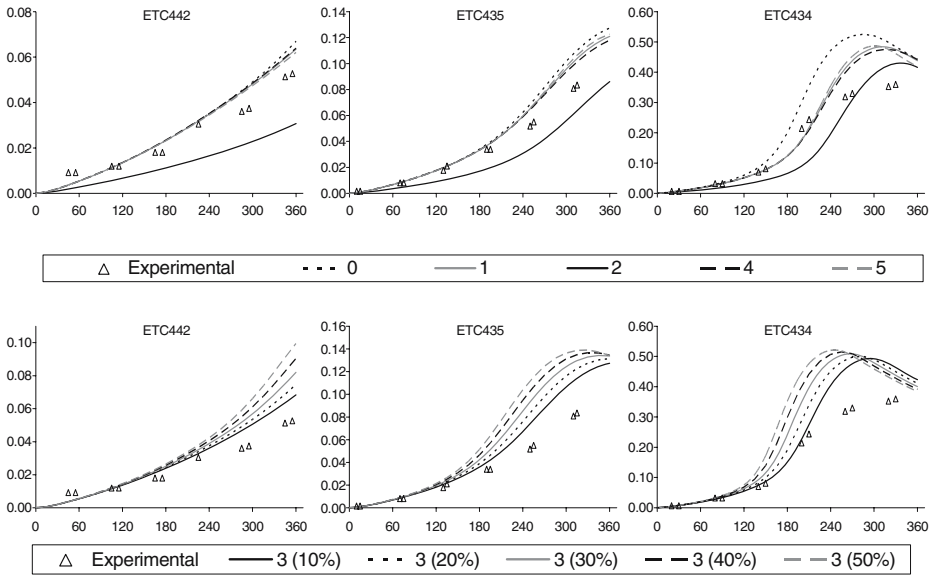

Fig. 12 Example plots of experimental and calculated HCHO (ppm) vs. time (min) for the β-pinene-NO_X - air experiments. ETC442-β-pinene/NO_X=0.946; ETC435-β-pinene/NO_X=2.018; ETC434-β-pinene/NO_X= 3.301. Legend: *numbers* correspond to mechanistic variations tested, see Table 4. For mechanism 3, the *numbers inside brackets* correspond to percentage of isomerisation of BPINAO

in some cases. Similarly to the α-pinene system, the sensitivity of the system to a number of mechanistic variations was tested, as listed in Table 4.

4.3.1 Variations in radical propagation pathways to first generation products

Sensitivity to variations in the initial distribution of peroxy radicals following attack of OH was initially considered. Particular emphasis was placed on simulations using a peroxy radical distribution of (0.435: 0.13: 0.435) for BPINAO2: BPINBO2: BPINCO2, such that formation of BPINCO2 was greatly increased compared with the base case (i.e., from 7.5 to 43.5%). These fractions were inferred from the results of the α-pinene appraisal of Peeters et al. (2001), discussed above in Section 4.2.4, which predicted an equal propensity for formation of the analogous structures APINAO2 and APINCO2 in that system. In contrast to the corresponding change in the α-pinene system, increasing the formation of BPINCO2 in the β-pinene system was found to lead to a notable decrease in $D(O_3–NO)$ formation and β-pinene decay in all experiments (see Figs. 9, 10 and 11, Mechanism 2). This is a direct consequence of the reduced formation of HCHO as a first generation product which, along with nopinone, derives entirely from the subsequent chemistry of BPINAO2 and BPINBO2 (see Fig. 1). The photolysis of HCHO leads to significant secondary radical generation, such that reducing its yield lowers the simulated reactivity of the system. The impact on the yield of HCHO was the overriding influence in tested modifications to the initiation branching ratios, with the greater number of NO-to-NO_2 conversions in the propagation sequence initiated by BPINCO2 (compared with BPINAO2 and BPINBO2) having a smaller compensating effect.

Vereecken and Peeters (2004) calculated that BPINCO2 also potentially undergoes a ring closure reaction, via internal addition to the double bond, with an estimated rate constant of 2.5 s^{-1}. This process was therefore also implemented, using a reaction sequence analogous

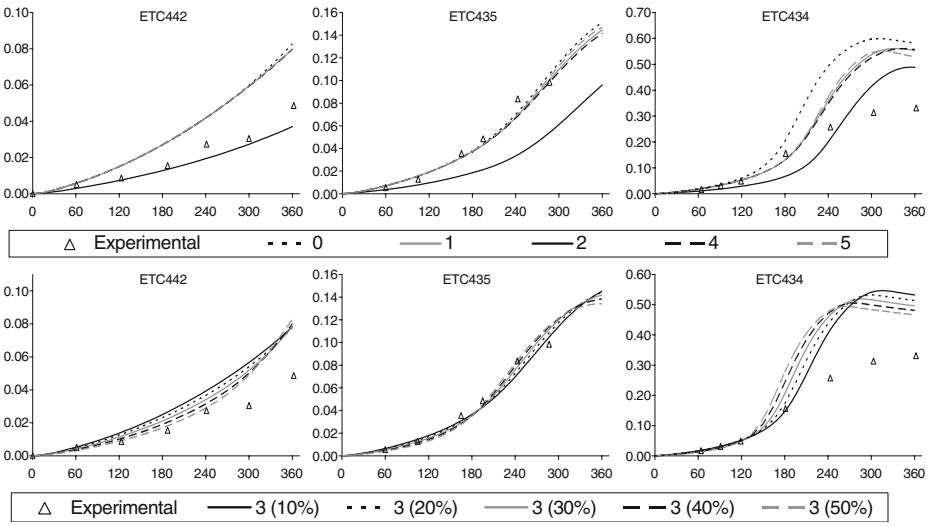

Fig. 13 Example plots of experimental and calculated nopinone (ppm) vs. time (min) for the β-pinene-NO_X -air experiments. ETC442-β-pinene/NO_X=0.946; ETC435-β-pinene/NO_X=2.018; ETC434-β-pinene/NO_X= 3.301. Legend: *numbers* correspond to mechanistic variations tested, see Table 4. For mechanism 3, the *numbers inside brackets* correspond to percentage of isomerisation of BPINAO

to that described for APINCO2 above (i.e., reaction sequence (20) and associated chemistry). For the conditions of the chamber experiments, inclusion of this chemistry was found to have only a very subtle effect in comparison with the effect of modifying the initiation branching ratios and the associated impact on HCHO.

4.3.2 Other pathways forming formaldehyde

Davis et al. (2005) have considered the possible participation of a competing 1,5-H atom shift isomerisation reaction for BPINAO, in relation to its impact on OH recycling in the OH-initiated oxidation of β-pinene. The postulated mechanism, which is entirely analogous to that discussed above for APINAO (i.e., reaction sequence (30) and associated chemistry), also provides and alternative route to formation of HCHO without formation of nopinone as a co-product. An explicit representation of this mechanism was implemented into Mechanism 1, with the contribution of the isomerisation reaction varied. As shown in Figs. 9, 10, 11, 12 and 13 (Mechanism 3), increasing the importance of the isomerisation reaction substantially increases the reactivity of the system by virtue of the three additional NO-to-NO_2 conversions in the corresponding mechanism, with the simulated formation rates of D(O_3–NO) and HCHO, and decay rate of β-pinene, increasing. As a result, inclusion of isomerisation as a partial fate for BPINAO (i.e., up to ca. 10–20%) leads to an improved agreement with observation in the higher VOC/NO_X experiments, but a poorer comparison with the experimental data in the lower VOC/NO_X experiments. However, increasing the importance of BPINAO isomerisation improves the agreement between simulated and observed nopinone in three of the four experiments for which data are available.

4.3.3 Variation of the attack distribution of OH on nopinone

The OH-initiated degradation of nopinone in MCM v3.1 is assumed to proceed via four H-abstraction channels, initially forming the 3-nopinonyl (13.6%), 4-nopinonyl (53.5%), 5-nopinonyl (13.0%) and 7-nopinonyl (19.9%) peroxy radicals. As indicated in Section 3, these reactions mainly initiate NO_X-propagated reaction sequences containing several NO-to-NO_2 conversions, but with the 4-nopinonyl route partially proceeding via a short reaction sequence, in which the 4-nopinonoxy radical reacts with O_2 (with a probability of ca. 40%) to generate the comparatively unreactive bicyclic diketone product 6,6-dimethyl-bicyclo [3.1.1]heptane-2,4-dione and HO_2. Lewis et al. (2005) have recently carried out a detailed theoretical appraisal of the OH-initiated attack distribution on nopinone, considering H atom abstraction from the seven possible positions. Of these, the routes considered in MCM v3.1 account for ca. 71% of the total, although the relative distribution differs considerably. The majority of the remaining attack (23.4%) was calculated by Lewis et al. (2005) to occur at the bridgehead adjacent to the carbonyl group to generate the 1-nopinonyl peroxy radical. A revised distribution was therefore implemented into Mechanism 1, based on that calculated by Lewis et al. (2005), but with the 1-nopinonyl contribution represented by attack at the other bridgehead position to form 5-nopinonyl for which the subsequent chemistry is similar. After minor scaling to all channel contributions to bring the total to 100%, the applied revised distribution was: 3-nopinonyl (47.0%), 4-nopinonyl (13.9%), 5-nopinonyl (35.5%) and 7-nopinonyl (3.6%). Because of the lowering of the 4-nopinonyl contribution, a main effect of implementing the revised distribution is to increase slightly the average chain length associated with nopinone oxidation. As shown in Figs. 9 and 11 (Mechanism 4), this led to very small increases in D(O_3–NO) in the lower VOC/NO_X experiments (e.g., ETC442) by virtue of the increased number of NO-to-NO_2 conversions;

but also slightly reduced D(O_3–NO) in the latter stages of the higher VOC/NO_X experiments (e.g., ETC434), resulting from the increased sequestration of NO_X in the form of organic oxidised nitrogen (e.g., a number of complex PAN species formed in the 3-nopinonyl route) under highly NO_X-limited conditions. Simulations were also carried out with OH attack assumed to proceed entirely via the 4-nopinonyl route, and with 4-nopinonoxy radical artificially assumed to react exclusively with O_2, thereby forcing the mechanism through the shortest reaction sequence. Accordingly, this resulted in small decreases in D(O_3–NO) in the lower VOC/NO_X experiments, and increased D(O_3–NO) in the latter stages of the higher VOC/NO_X experiments (Figs. 9 and 11, Mechanism 5). It is emphasised, however, that the rate of D(O_3–NO) formation and β-pinene removal for the conditions of these experiments is comparatively insensitive to changes in the OH attack distribution on nopinone.

5 Discussion and conclusions

5.1 α-pinene/NO_X system

The results presented in Section 4.2 demonstrate that MCM v3.1 provides a consistent description of photo-oxidation of α-pinene/NO_X mixtures for a range of initial VOC/NO_X, but with the formation rate of ozone and decay rate of α-pinene generally being overestimated. Sensitivity tests indicated that the implementation of a series of sequential changes to the mechanism allowed the simulations to be brought into very good agreement with observations, with the resultant mechanism providing a good description of ozone formation for quantity of α-pinene removed in the complete series of experiments. As with our previous evaluations of isoprene and alkene oxidation (Pinho et al. 2005, 2006), the system was particularly sensitive to the applied magnitudes of sources and sinks for free radicals, and many of the implemented changes were designed either to decrease radical input (i.e., through reducing secondary radical formation from pinonaldehyde photolysis and the radical yield from α-pinene ozonolysis), or to increase radical removal (i.e., through increasing the first generation yield of nitrates from the reactions of RO_2 with NO). In addition, a notable improvement in the latter stages of the simulations resulted from revisions made to the OH-initiated degradation mechanism for pinonaldehyde, informed by the theoretical appraisal of Fantechi et al. (2002), which had the main effect of significantly reducing the associated oxidation chain length (i.e., the number of NO-to-NO_2 conversions).

The simulations were found to be generally insensitive to modifications made to the first generation propagation routes, provided these did not significantly change the nitrate yields, the number of NO-to-NO_2 conversions or the reactivity/photolability of the product distribution. As a result, the associated mechanistic refinements based on the appraisals of Peeters and co-workers (described in Section 4.2.4) had only a subtle influence on the simulations of oxidant formation and α-pinene decay. Nevertheless, it is recognised that such mechanistic changes do influence the precise product distribution, and may therefore have much greater effects on assessments of impacts other than ozone formation (e.g., the propensity of products to contribute to secondary organic aerosol formation). In addition, it is noted that the adjustments generally decreased the formation of pinonaldehyde from the OH-initiated chemistry, leading to effective yields which are reduced towards the lower values reported in several studies (see Section 3). However, this aspect of the mechanism could not be tested directly, because pinonaldehyde observations were unavailable for the considered chamber experiments.

Although the applied sequential revisions made to the mechanism are all consistent with the literature, it was necessary to set the revised first generation nitrate yields (27%) and the revised yield of OH and its co-radical(s) from α-pinene ozonolysis (70%) at the extremities of reported values or uncertainty ranges. It is recognised that this may be compensating for other uncertainties and/or omissions in the α-pinene mechanism. In this respect, the revised mechanism was unable to recreate the magnitude of observed HCHO formation, leading to an underestimation in all experiments. Implementation of postulated routes to HCHO formation could not account for the discrepancies, within the framework of the mechanism. This is partially because the HCHO-forming routes are accompanied by additional NO-to-NO_2 conversion steps (particularly the mechanism involving isomerisation of APINAO or similar routes), leading to significant additional ozone formation. In addition, any increase in simulated HCHO formation has an intrinsic knock-on effect on ozone formation through increased secondary radical generation from HCHO photolysis. Consequently, correct representation of HCHO formation (even if this is accompanied by no additional NO-to-NO_2 conversion steps) would actually require further compensating refinements to be made to parameter values or other aspects of the mechanism to allow the overall reactivity of the system to be maintained. It is noted, however, that the implementation of any of the HCHO formation routes once again serves to lower the effective yield of pinonaldehyde from the OH-initiated chemistry.

5.2 β-pinene/NO_X system

The results presented in Section 4.3 indicate that MCM v3.1 provides a reasonable, but less consistent, description of photo-oxidation of β-pinene/NO_X mixtures. Although the simulated magnitudes of the ozone formation rates and β-pinene removal rates were broadly comparable with the experimental observations, the mechanism tends towards overestimation of ozone formation at low VOC/NO_X and underestimation at high VOC/NO_X. A number of mechanistic variations reported in the literature were tested, but it was not possible bring the associated simulations into good agreement with the observations for the entire VOC/NO_X range. The system was found to be particularly sensitive to changes which influenced the formation of HCHO, and the impacts of the tested mechanistic variations were usually dominated by this effect.

The simulations were found to be generally insensitive to modifications made to the OH attack distribution on the first generation product nopinone, although it is recognised that the timescale and conditions of the considered experiments primarily provide a test for the initial oxidation step (the system being of lower reactivity than α-pinene). Changes to the OH attack distribution not only influence the number of NO-to-NO_2 conversions during nopinone degradation, but also the precise product distribution and may therefore have notable effects on assessments of impacts other than ozone formation at greater extents of chemical processing. For example, the 3-nopinonyl route (favoured in the appraisal of Lewis et al. 2005) feeds directly into accepted mechanisms generating pinic acid (e.g., Jenkin et al. 2000; Winterhalter et al. 2000), which is believed to contribute to secondary organic aerosol formation in the pinene systems.

As indicated above, the observed cessation of chemical processing after ca. 200 minutes in the highest VOC/NO_X experiment (ETC434) could only be recreated by inclusion of an efficient artificial sink for NO_X becoming active at the appropriate point. Although the precise nature of the process could not be determined, one possibility is photo-enhanced uptake of NO_2 on newly-formed secondary organic aerosol (e.g., George et al. 2005).

5.3 Recommendations

As a result of this work, it is possible to make a number of suggestions and recommendations for future work, in relation to gaps and uncertainties in the kinetic, mechanistic and chamber database.

- Further studies are required to reduce the uncertainties in key parameters related to sources and sinks of free radicals in the initial oxidation steps, as discussed above. In particular, there is only limited information on the first generation yields of organic nitrates, the formation of which is accompanied by radical removal. Although the yields of OH (and co-radicals) from the ozonolysis of α- and β-pinene have been reported in a number of studies, these have generally been derived from experiments performed in the absence of NO_X. It is therefore not clear to what extent the presence of NO_X influences the mechanisms forming OH (and/or other radicals).
- Despite considerable investigation, the distribution of first generation products of α-pinene and β-pinene oxidation, and the elementary processes leading to their formation, remain far from fully characterised. There is some uncertainty in the routes to formation of HCHO as a first generation product of α-pinene degradation (and in its yield and formation mechanism from the further degradation of pinonaldehyde). Identification and characterisation of the supplementary mechanisms forming HCHO from β-pinene degradation are also required.
- More experimental information is also required on the elementary processes occurring in the further degradation of first generation products of α-pinene and β-pinene oxidation, such as pinonaldehyde and nopinone, but also a number of other identified and unidentified multifunctional products. In addition, chamber datasets for the product compounds (and possibly their degradation products) would be valuable in assessing the performance of mechanisms such as the MCM, and for gaining insights into chemical processes occurring on timescales longer than those addressed by conventional chamber experiments. This is particularly important for large complex emitted VOC, which are typically degraded via a large number of sequential (and parallel) steps.

Acknowledgments PP gratefully acknowledges support from the Departamento de Ambiente da Escola Superior de Tecnologia de Viseu, for providing time and material conditions to carry out this research. MEJ gratefully acknowledges support from the UK Natural Environment Research Council (NERC), via provision of a Senior Research Fellowship (NER/K/S/2000/00870 and NE/D008794/1), and from the UK Department for Environment, Food and Rural Affairs, DEFRA, AEQ Division (under contract EPG 1/3/200).

References

Alvarado, A., Tuazon, E.C., Aschmann, S.M., Atkinson, R., Arey, J.: Product of the gas phase reactions of $O(^3P)$ atoms and O_3 with α-pinene and 1,2-dimethyl-1-cyclo-hexene. J. Geophys. Res. **103**, 25541–25551 (1998)

Arey, J., Atkinson, R., Aschmann, S.M.: Product study of the gas-phase reactions of monoterpenes with the OH radical in the presence of NO_x. J. Geophys. Res. **95**, 18539–18546 (1990)

Aschmann, S.M., Reissell, A., Atkinson, R., Arey, J.: Products of the gas phase reactions of the OH radical with α- and β-pinene in the presence of NO. J. Geophys. Res. – Atmospheres **103**(D19), 25553–25561 (1998)

Aschmann, S.M., Arey, J., Atkinson, R.: Atmospheric chemistry of three C_{10} alkanes. J. Phys. Chem. **105**, 7598–7606 (2001)

Aschmann, S.M., Arey, J., Atkinson, R.: Products of reaction of OH radicals with α-pinene. J. Geophys. Res. – Atmospheres **107**(D14), 4191 (2002a), doi:10.1029/2001JD001098

Aschmann, S.M., Arey, J., Atkinson, R.: OH radical formation from the gas-phase reactions of O_3 with a series of terpenes. Atmos. Environ. **36**, 4347–4355 (2002b)

Atkinson, R.: Atmospheric chemistry of VOCs and NOx. Atmos. Environ. **34**, 2063–2101 (2000)

Atkinson, R., Aschmann, S.M., Arey, J., Shorees, B.: Formation of OH radicals in the gas-phase reactions of O_3 with a series of terpenes. J. Geophys. Res. **97**, 6065–6073 (1992)

Atkinson, R., Baulch, D.L., Cox, R.A., Crowley, J.N., Hampson, R.F., Hynes, R.G., Jenkin, M.E., Rossi, M. J., Troe, J.: Evaluated kinetic and photochemical data for atmospheric chemistry. Volume II: Reactions of organic species. Atmos. Chem. Phys. **6**, 1461–1738 (2006)

Berndt, T., Böge, O., Stratmann, F.: Gas-phase ozonolysis of α-pinene: gaseous products and particle formation. Atmos. Environ. **37**, 3933–3945 (2003)

Bloss, C., Wagner, V., Jenkin, M.E., Volkamer, R., Bloss, W.J., Lee, J.D., Heard, D.E., Wirtz, K., Martin-Reviejo, M., Rea, G., Wenger, J.C., Pilling, M.J.: Development of a detailed chemical mechanism (MCMv3.1) for the atmospheric oxidation of aromatic hydrocarbons. Atmos. Chem. Phys. **5** 641–644 (2005)

Bonn, B., von Kuhlmann, R., Lawrence, M.G.: High contribution of biogenic hydroperoxides to secondary organic aerosol formation. Geophys. Res. Lett. **31**, L10108 (2004), doi:10.1029/2003GL019172

Calvert, J.G., Atkinson, R., Kerr, J.A., Madronich, S., Moortgat, G.K., Wallington, T.J., Yarwood, G.: The Mechanisms of Atmospheric Oxidation of Alkenes. Oxford University Press, New York (2000), ISBN 0195131770

Capouet, M., Peeters, J., Nozière, B., Müller, J.F.: Alpha-pinene oxidation by OH: Simulations of laboratory experiments. Atmos. Chem. Phys. **4**, 2285–2311 (2004)

Carter, W.P.L.: Documentation of the SAPRC-99 chemical mechanism for VOC reactivity assessment. Final Report to California Air Resources Board Contract 92-329 and Contract 95-308, Air Pollution Research Center and College of Engineering Center for Environmental Research and Technology University of California Riverside, California. Available at http://www.cert.ucr.edu/~carter/absts.htm#saprc99 and http://www.cert.ucr.edu/~carter/reactdat.htm (2000)

Carter, W.P.L., Lurmann, F.W.: Evaluation of a detailed gas-phase atmospheric reaction mechanism using environmental chamber data. Atmos. Environ. **25A**, 2771–2806 (1991)

Carter, W.P.L., Luo, D., Malkina, I.L., Fitz, D.: The University of California, Riverside Environmental Chamber Data Base for Evaluating Oxidant Mechanisms: Indoor Chamber Experiments Through 1993. EPA/600/SR-96/078, U.S. Environmental Protection Agency, Research Triangle Park, NC. Available at http://www.cert.ucr.edu/~carter/absts.htm#databas (1995a)

Carter, W.P.L., Luo, D., Malkina, I.L., Pierce, J.A.: Environmental Chamber Studies of Atmospheric Reactivities of Volatile Organic Compounds. Effects of Varying Chamber and Light Source. Final report to National Renewable Energy Laboratory, Contract XZ-2-12075, Coordinating Research Council, Inc., Project M-9, California Air Resources Board, Contract A032-0692, and South Coast Air Quality Management District, Contract C91323. Available at http://www.cert.ucr.edu/~carter/absts.htm#explrept (1995b)

Chew, A.A., Atkinson, R.: OH radical formation yields from the gas-phase reactions of O_3 with alkenes and monoterpenes. J. Geophys. Res. **101**, 28649–28653 (1996)

Cvetanovic, R.J.: Evaluated chemical kinetic data for the reactions of atomic oxygen $O(^3P)$ with unsaturated hydrocarbons. J. Phys. Chem. Ref. Data **16**, 261–326 (1987)

Davis, M.E., Stevens, P.S.: Measurements of the kinetics of the OH-initiated oxidation of alpha-pinene: Radical propagation in the OH + alpha-pinene + O_2 + NO reaction system. Atmos. Environ. **39**, 1765–1774 (2005)

Davis, M.E., Tapscott, C., Stevens, P.S.: Measurements of the kinetics of the OH-initiated oxidation of β-pinene: Radical propagation in the OH + β-pinene + O_2 + NO reaction system. Int. J. Chem. Kinet. **37**, 522–531 (2005)

Derwent, R.G., Jenkin, M.E., Saunders, S.M., Pilling, M.J., Passant, N.R.: Multi-day ozone formation for alkenes and carbonyls investigated with a master chemical mechanism under European conditions. Atmos. Environ. **39**, 625 (2005)

Fantechi, G., Vereecken, L., Peeters, J.: The OH-initiated atmospheric oxidation of pinonaldehyde: Detailed theoretical study and mechanism construction. Phys. Chem. Chem. Phys. **4**, 5795–5805 (2002)

Finlayson-Pitts, B.J., Pitts, J.N. Jr.: Chemistry of the Upper and Lower Atmosphere. Academic, San Diego (2000)

George, C., Strekowski, R.S., Kleffmann, J., Stemmler, K., Ammann, M.: Photoenhanced uptake of gaseous NO_2 on solid organic compounds: a photochemical source of HONO? Faraday Discuss. **130**, 195–210 (2005)

Gierczak, T., Burkholder, J.B., Bauerle, S., Ravishankara, A.R.: Photochemistry of acetone under tropospheric conditions. Chem. Phys. **231**, 229–244 (1998)

Gu, C.L., Rynard, C.M., Hendry, D.G., Mill, T.: OH Radical Oxidation of α-pinene. Report to US Environmental Protection Agency, Grant R8081-10010, SRI International, Menlo Park, CA (1984)
Guenther, A.B., Zimmerman, P., Wildermuth, M.: Natural volatile organic compound emission rate estimates for U.S. woodland landscapes. Atmos. Environ. **28**, 1197–1210 (1994)
Guenther, A.B., Hewitt, C.N., Erickson, D., Fall, R., Geron, C., Graedel, T., Harley, P., Klinger, L., Lerdau, M., McKay, W.A., Pierce, T., Scholes, B. Steinbrecher, R., Tallamraju, R., Taylor, J., Zimmerman, P.: A global model of natural volatile organic compound emissions. J. Geophys. Res. **100**, 8873–8892 (1995)
Hakola, H., Arey, J., Aschmann, S.M., Atkinson, R.: Product formation from the gas-phase reactions of OH radicals and O_3 with a series of monoterpenes. J. Atmos. Chem. **18**, 75–102 (1994)
Hatakeyama, S., Izumi, K., Fukuyama, T., Akimoto, H.: Reactions of OH with α-pinene and β-pinene in air, estimate of global CO production from the atmospheric oxidation of terpenes. J. Geophys. Res. **96**, 947–958 (1991)
Hynes, R.G., Angove, D.E., Saunders, S.M., Haverd, V., Azzi, M.: Evaluation of two MCM v3.1 alkene mechanisms using indoor environmental chamber data. Atmos. Environ. **39**, 7251–7262 (2005)
Jenkin, M.E.: Analysis of sources and partitioning of oxidant in the UK – part 1: the NOx -dependence of annual mean concentrations of nitrogen dioxide and ozone. Atmos. Environ. **38**, 5117–5129 (2004)
Jenkin, M.E., Clemitshaw, K.C.: Ozone and other secondary photochemical pollutants: chemical processes governing their formation in the planetary boundary layer. Atmos. Environ. **34**, 2499–2527 (2000)
Jenkin, M.E., Saunders, S.M., Pilling, M.J.: The tropospheric degradation of volatile organic compounds: a protocol for mechanism development. Atmos. Environ. **31**, 81–104 (1997)
Jenkin, M.E., Shallcross, D.E., Harvey, J.N.: Development and application of a possible mechanism for the formation of cis-pinic acid from the ozonolysis of α- and β-pinene. Atmos. Environ. **34**, 2837–2850 (2000)
Jenkin, M.E., Saunders, S.M., Derwent, R.G., Pilling, M.J.: Development of a reduced speciated VOC degradation mechanism for use in ozone models. Atmos. Environ. **36**, 4725–4734 (2002)
Jenkin, M.E., Saunders, S.M., Wagner, V., Pilling, M.J.: Protocol for the development of the Master Chemical Mechanism, MCM v3, Part B: tropospheric degradation of aromatic volatile organic compounds. Atmos. Chem. Phys. **3**, 181–193 (2003)
Jenkin, M.E., Andersen, M.P.S., Hurley, M.D., Wallington, T.J., Taketani, F., Matsumi, Y.: A kinetics and mechanistic study of the OH and NO_2 initiated oxidation of cyclohexa-1,3-diene in the gas phase. Phys. Chem. Chem. Phys. **7**, 1194–1204 (2005)
Johnson, D., Utembe, S.R., Jenkin, M.E., Derwent, R.G., Hayman, G.D., Alfarra, M.R., Coe, H., McFiggans, G.: Simulating regional scale secondary organic aerosol formation during the TORCH 2003 campaign in the southern UK. Atmos. Chem. Phys. **6**, 403–418 (2006a)
Johnson, D., Utembe, S.R., Jenkin, M.E.: Simulating the detailed chemical composition of secondary organic aerosol formed on a regional scale during the TORCH 2003 campaign in the southern UK. Atmos. Chem. Phys. **6**, 419–431 (2006b)
Kesselmeier, J.K., Staudt, M.: Biogenic volatile organic compounds (VOC): An overview on emission, physiology and ecology. J. Atmos. Chem. **33**, 23–88 (1999)
Leighton, P.A.: Photochemistry of Air Pollution. Academic, New York (1961)
Lewis, P.J., Bennett, K.A., Harvey, J.N.: A computational study of the atmospheric oxidation of nopinone. Phys. Chem. Chem. Phys. **7**, 1643–1649 (2005)
Martinez, R.D., Buitrago, A.A., Howell, N.W., Hearn, C.H.G., Joens, J.A.: The near UV absorption spectra of several aliphatic aldehydes and ketones at 300 K. Atmos. Environ. **26A**, 785–792 (1992)
Meyrahn, H., Pauly, J., Scheneider, W., Warneck, P.: Quantum yields for the photodissociation of acetone in air and an estimate for the life time of acetone in the lower troposphere. J. Atmos. Chem. **4**, 277–291 (1986)
Nozière, B., Barnes, I., Becker, K.: Product study and mechanisms of the reactions of α-pinene and of pinonaldehyde with OH radicals. J. Geophys. Res. **104**, 23645–23658 (1999)
O'Brien, J.M., Czuba, E., Hastie, D.R., Francisco, J.S., Shepson, P.B.: Determination of the hydroxy nitrate yields from the reaction of C_2–C_6 alkenes with OH in the presence of NO. J. Phys. Chem. A **102**, 8903–8908 (1998)
Orlando, J., Nozière, B., Tyndall, G., Orzechowska, G., Paulson, S., Rudich, Y.: Product studies of the OH- and ozone-initiated oxidation of some monoterpenes. J. Geophys. Res. **105**, 11561–11572 (2000)
Paulson, S.E., Chung, M., Sen, A.D., Orzechowska, G.: Measurement of OH radical formation from the reaction of ozone with several biogenic alkenes. J. Geophys. Res. **103**, 25533–25539 (1998)
Peeters, J., Boullart, W., Hoeymissen, J.V.: In: Proceedings of EUROTRAC Symposium 94, p 110. SPB Academic Publ., The Hague, The Netherlands (1994)
Peeters, J., Vereecken, L., Fantechi, G.: The detailed mechanism of the OH-initiated atmospheric oxidation of α-pinene: a theoretical study. Phys. Chem. Chem. Phys. **3**, 5489–5504 (2001)

Pinho, P.G., Pio, C.A., Jenkin, M.E.: Evaluation of isoprene degradation in the detailed tropospheric chemical mechanism, MCM v3, using environmental chamber data. Atmos. Environ. **39**, 1303–1322 (2005)

Pinho, P.G., Pio, C.A., Carter, W.P.L., Jenkin, M.E.: Evaluation of alkene degradation in the detailed tropospheric chemistry mechanism, MCM v3, using environmental chamber data. J. Atmos. Chem. **55**, 55–79 (2006)

PORG: Ozone in the United Kingdom. Fourth report of the UK Photochemical Oxidants Review Group, Department of the Environment, Transport and the Regions, London. Published by Institute of Terrestrial Ecology, Bush Estate, Penicuik, Midlothian, EH26 0QB, UK. ISBN:0-870393-30-9, available at 'http://www.aeat.co.uk/netcen/airqual/reports/home.html' (1997)

Poschl, U., von Kuhlmann, R., Poisson, N., Crutzen, P.J.: Development and intercomparison of condensed isoprene oxidation mechanisms for global atmospheric modelling. J. Atmos. Chem. **37**, 29–52 (2000)

RADICAL: Final report on the EU fourth framework project 'evaluation of radical sources in atmospheric chemistry through chamber and laboratory studies, RADICAL.'European Communities Report EUR 20254 EN, G. K. Moortgat (Coordinator). MPI Mainz, Germany (2002)

Rickard, A.R., Johnson, D., McGill, C.D., Marston, G.: OH yields in the gas-phase reactions of ozone with alkenes. J. Phys. Chem. A **103**, 7656–7664 (1999)

Ruppert, L., Becker, K.H., Nozière, B., Spittler, M.: Development of monoterpene oxidation mechanisms: results from laboratory and smog chamber studies. Borrell, P.M., Borrell, P. (eds.) Transport and Chemical Transformation in the Troposphere. Proceedings of the EUROTRAC-2 Symposium '98, pp. 63–68. WIT, Southampton, UK (1999)

Saunders, S.M., Jenkin, M.E., Derwent, R.G., Pilling, M.J.: Protocol for the development of the Master Chemical Mechanism, MCM v3, part A: tropospheric degradation of non-aromatic volatile organic compounds. Atmos. Chem. Phys. **3**, 161–180 (2003)

Siese, M., Becker, K.H., Brockmann, K.J., Geiger, H., Hofzumahaus, A., Holland, F., Mihelcic, D., Wirtz, K.: Direct measurement of OH radicals from ozonolysis of selected alkenes: a EUPHORE simulation chamber study. Environ. Sci. Technol. **35**, 4660–4667 (2001)

Tadic, J., Juranic, I., Moortgat, G.K.: Pressure dependence of the photooxidation of selected carbonyl compounds in air: n-butanal and n-pentanal. J. Photochem. Photobiol., A Chem. **143**, 169–179 (2001a)

Tadic, J., Juranic, I., Moortgat, G.K.: Photooxidation of *n*-hexanal. Molecules **6**, 287–299 (2001b)

Tadic, J.M., Juranic, I.O., Moortgat, G.K.: Photooxidation of *n*-heptanal in air: Norrish type I and II processes and quantum yield total pressure dependency. J. Chem. Soc., Perkin Trans. **2**, 135–140 (2002)

Utembe, S.R., Jenkin, M.E., Derwent, R.G., Lewis, A.C., Hopkins, J.R., Hamilton J.F.: Modelling the ambient distribution of organic compounds during the August 2003 ozone episode in the southern UK. Faraday Discuss. **130**, 311–326 (2005)

Vereecken, L., Peeters, J.: Theoretical study of the formation of acetone in the OH-initiated atmospheric oxidation of α-pinene. J. Phys. Chem. A **104**, 11140–11146 (2000)

Vereecken, L., Peeters, J.: Non-traditional (per)oxy ring-closure paths in the atmospheric oxidation of isoprene and monoterpenes. J. Phys. Chem. A **108**, 5197–5204 (2004)

Warneck, P.: Photodissociation of acetone in the troposphere: an algorithm for the quantum yield. Atmos. Environ. **35**, 5773–5777 (2001)

Whitehouse, L.E., Tomlin, A.S., Pilling, M.J.: Systematic reduction of complex tropospheric chemical mechanisms, part I: sensitivity and time-scale analyses. Atmos. Chem. Phys. **4**, 2025–2056 (2004a)

Whitehouse, L.E., Tomlin, A.S., Pilling, M.J.: Systematic reduction of complex tropospheric chemical mechanisms, part II: lumping using a time-scale based approach. Atmos. Chem. Phys. **4**, 2057–2081 (2004b)

Winterhalter, R., Neeb, P., Grossmann, D., Kolloff, A., Horie, O., Moortgat, G.K.: Products and mechanism of the gas-phase reaction of ozone with β-pinene. J. Atmos. Chem. **35**, 165–197 (2000)

Wisthaler, A., Jensen, N.R., Winterhalter, R., Lindinger, W., Hjorth, J.: Measurements of acetone and other gas phase product yields from the OH-initiated oxidation of terpenes by Proton-Transfer-Reaction Mass Spectrometry (PTR-MS). Atmos. Environ. **35**, 6151–6191 (2001)

Zádor, J., Wagner, V., Wirtz, K., Pilling, M.J.: Quantitative assessment of uncertainties for a model of tropospheric ethene oxidation using the European Photoreactor (EUPHORE). Atmos. Environ. **39**, 2805–2817 (2005)